



# Debris flow susceptibility mapping using the Rock Engineering System (RES) method: a case study

**Abstract** The main purpose of the present study is to develop a debris flow susceptibility map of a mountain area (Susa Valley, Western Italian Alps) by using an upgraded version of the Bonetto et al. (*Journal of Mountain Science* 18, 2021) approach based on the Rock Engineering System (RES) method. In particular, the area under investigation was discretized in a  $5 \times 5$ -m grid on which GIS-based analyses were performed. Starting from available databases, several geological, geo-structural, morphological and hydrographical predisposing parameters were identified and codified into two interaction matrices (one for outcropping lithologies and one for Quaternary deposits), to evaluate their mutual interactions and their weight in the susceptibility estimation. The result for each grid point is the debris flow propensity index (DfPI), an index that estimates the susceptibility of the cell to be a potential debris flow source. The debris flow susceptibility map obtained was compared with those obtained from two expedited and universally recognized susceptibility methods, i.e. the Regional Qualitative Heuristic Susceptibility Mapping (RQHSM) and the Likelihood Ratio (LR). Each map was validated by using the Prediction Rate Curve method. The limitations and strong points of the approaches analysed are discussed, with a focus on the innovativeness and uniqueness of the RES. In fact, in the study site, the RES method was the most efficient for the detection of potential source areas. These results prove its robustness, cost-effectiveness and speed of application in the identification and mapping of sectors capable of triggering debris flow.

**Keywords** Rock Engineering System (RES) · Debris flow susceptibility · Susceptibility mapping · Open source data

## Introduction

Debris flows are rapid landslides of mixed and unconsolidated sediments and water which occur when soil and rock fragments become saturated and flow down into a steep channel driven by the force of gravity. Debris flow events can be extremely dangerous for humans and infrastructures due to their high velocity (up to 20 m/s), their large mobilized volumes (even more than  $10^9$  m<sup>3</sup>) and their unpredictability (Varnes 1978; Hutchinson 1988; IAEG 1990; Cruden and Varnes 1996). A careful territorial analysis should include the identification of potential debris flow source areas for correct land use and risk management, especially in mountain regions where these aspects become fundamental for the resilience of the rural areas and to tackle the effects of climate change.

Geological, geomorphological, hydrogeological and landslide maps (Soeters and Van Westen 1996; Fell et al. 2008; Corominas et al. 2014), supported by direct field observations, are fundamental to detect and delimit zones susceptible to landslide triggering

(including debris flow). Several models have been proposed in the scientific literature for evaluating landslide susceptibility by combining geo-environmental factors and landslide spatial distribution (Brabb 1987; Soeters and van Westen 1996; Carrara et al. 1984, 1999, 2008; Aleotti and Chowdhury 1999; Guzzetti et al. 1999; Dai and Lee 2001; Chacón et al. 2006; Fell et al. 2008; Reichenbach et al. 2018). In general, these models are based on the identification of those factors that contribute to landslide triggering, by distinguishing between predisposing and triggering factors (e.g. Costa and Jarrett 1981; Hutchinson 1992; Cruden and Varnes 1996; Jakob and Hungr 2005; Hungr 2005; Van Westen et al. 2008; Pereira et al. 2012; Corominas et al. 2014; Iverson 2014, 1997; Hungr et al. 2014 and references herein). Data related to triggering factors represent an important set of input parameters for landslide hazard assessment, while the predisposing factors and landslide inventories play a key role in landslide susceptibility analysis (Dai and Lee 2001; Clerici et al. 2002; Corominas et al. 2003, 2014; Van Westen et al. 2006).

Susceptibility analysis can be assessed through both qualitative (inventory-based and knowledge-driven methods) and quantitative (data-driven methods and physically based models) methods (Carrara et al. 1995; Soeters and Van Westen 1996; Guzzetti et al. 1999, 2006a, b; Dai and Lee 2001; Van Westen et al. 2006; Clerici et al. 2002). Inventory-based methods provide a multitemporal landslide distribution (spatial and temporal frequencies) based on historical series and represent a key starting point for hazard mapping and risk assessment. The analysis of past debris flow events provides useful information for forecasting future debris flow, based on topographic, geological and geomorphologic characteristics. The knowledge-driven approaches, or heuristic methods, are based on the expert knowledge of landslide mechanisms that allows the degree of instability, combining geomorphological observations and thematic geological maps to be determined (Abella and Van Westen 2008; Nachbaur and Rohmer 2011). This approach can be applied when the landslide inventory is incomplete or when a preliminary and expedited evaluation is needed.

In data-driven landslide susceptibility methods, statistical and quantitative predictions are made using the records of past landslide events through three different approaches: bivariate, multivariate and active learning statistical analyses. Landslide distribution could define the functional relationships among known or inferred instability factors (Malusà and Mosca 2002; Guzzetti et al. 1999; Huabin et al. 2005; Chacón et al. 2006; van Westen et al. 2008), but results are strongly influenced by the quality and completeness of the inventory (Guzzetti et al. 2006a, b; Reichenbach et al. 2018).

The physically based models are based on the mathematical modelling of landslide failure and a set of numerical parameters that

describe the geometry, and the internal and external slope condition. Slope analysis can be done using simple limit equilibrium models, such as the infinite slope model, or more complex approaches like kinematics analysis or numerical modelling (Montgomery and Dietrich 1994; Rigon et al. 2006; van Asch et al. 2007; Simoni et al. 2008; Baum and Godt 2010; Anagnostopoulos and Burlando 2012; Alvioli and Baum 2016).

For susceptibility mapping purposes, the choice of the methods should be driven by the availability of the input parameters required for the analyses and their mutual interactions. Recently, Bonetto et al. (2021) proposed an application of the Rock Engineering System (RES; Hudson 1992) to debris flows analysis. The RES approach has also been used for other landslide types (Mazzoccola and Hudson 1996; Kim et al. 2008; Rozos et al. 2008; Tavoularis et al. 2017, 2021; Xiao et al. 2020; Pokharel et al. 2021 and references herein) and implemented in neural network approaches (Wang et al. 2014; Meten et al. 2015). Bonetto et al. (2021) combined inventory, expert evaluation and data-driven methods for a quantitative evaluation of the debris flow propensity at a basin-scale RES methodology were then used to evaluate the Debris flow Propensity Index (DfPI) by quantifying and scoring the mutual interaction between predisposing parameters. Starting from these assumptions and promising results, in this paper, the authors propose an upgraded version of the Bonetto et al. (2021) methodology applied to debris flow by considering new parameters for the DfPI determination and by implementing the procedure in GIS environment. The predisposing parameters are encoded into two interaction matrixes to consider outcropping lithologies and Quaternary deposits and the DfPI values are mapped onto a 5 × 5-m grid cell resolution. The procedure has been tested on the same sector of the western Italian Alps (Upper Susa Valley) as in Bonetto et al. (2021) for a direct comparison and validation of the results.

The susceptibility map obtained is compared with those obtained by two methods available in the scientific literature: the Regional Qualitative Heuristic Susceptibility Mapping (RQHSM) method proposed by Soeters and van Westen (1996) and the Likelihood Ratio (LR) method (Lee 2004; Regmi et al. 2010; Sujatha et al. 2013; Kanungo et al. 2011; Akgun 2012). The limitations and strong points of the methodologies are discussed by comparing susceptible areas with an available debris flow source area database. Furthermore, the differences between the three methods are quantitatively assessed by using the “Prediction Rate Curve” method (Chung and Fabbri 2003).

### Study area: the Upper Susa Valley

The study area is the Upper Susa Valley, in the Western Italian Alps (Fig. 1A). Many basins of this valley are affected by recurrent debris flow events, which occurred especially during late summer and fall seasons (Tiranti et al. 2008, 2014, 2016). These phenomena have caused many damages to the crucial infrastructures, which link the valley (and more in general Turin) to France, and to the urbanized areas, which mainly developed on debris fans.

This valley is drained by the Dora Riparia River, a left-hand tributary of the Po River, and has been carved by glaciers at the end of Pleistocene in units belonging to the Penninic domain of the Western Alps.

The Western Alps result from the collision between European and Adriatic plates following subduction and closure of their interposed Piemonte-Liguria oceanic basin (e.g. Dal Piaz 2010a, b and therein references). The upper Susa Valley exposes a tectonic stack of continental margin (Ambin Massif Auct., Pre-Piedmont and Briançonnais units) and oceanic Piemonte-Liguria units (Fig. 1; Polino et al. 2002; Piana et al. 2017). The Ambin massif Auct. comprises two pre-alpine complexes: the Clarea and the Ambin complexes, resting at lower and

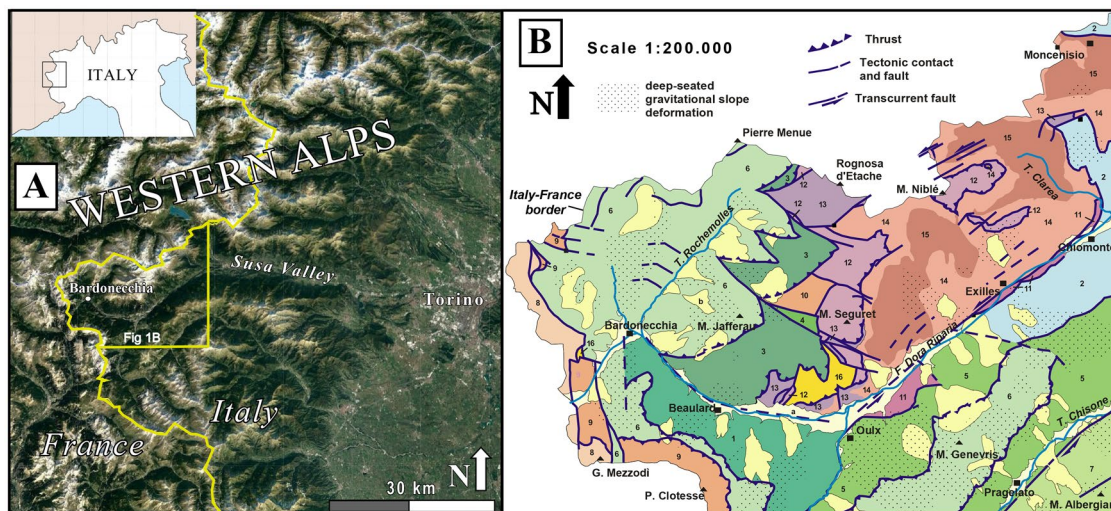


**Fig. 1** A Location of the Susa Valley in the Italian Western Alps (© Google Maps). B Tectonic sketch map of the Upper Susa Valley (from Servizio Geologico d'Italia 2002). Legend: 1—Puys Complex; 2—Venaus Complex; [Oceanic units] 3—Aigle Unit; 4—Vin Vert Unit; 5—Cerogne-Ciantiplagna Unit; 6—Lago Nero Unit; 7—Albergian Unit;

[Continental margin units] 8—Re Magi Unit; 9—Chaberton-Grand Hoche-Grand Argentier unit; 10—Valfreda Unit; 11—Gad Unit; 12—Vallonetto Unit; 13—Permo-mesozoic succession of the Ambin Complex; 14—Ambin Complex; 15—Clarea Complex; 16—Gypsum and tectonic carbonate breccias; a - alluvial deposits; b - major landslide

upper structural levels respectively (Polino et al. 2002; Malusà et al. 2002; Malusà and Mosca 2002). The Clarea complex consists of micaschist and paragneiss embedding metabasite and orthogneiss of dioritic composition. The Ambin complex is formed by gneiss and quartz-micaschist derived from volcanoclastic protoliths, several types of micaschist and bodies of aplitic gneiss. This complex is overlaid by a Permo-Mesozoic cover consisting of conglomeratic quartzite with pink quartz clasts and levels of sericitic schist (upper Permian), massive quartzite (lower Triassic) and a succession of dolomitic marbles and calcareous schists with local intercalation of carbonate breccias (Triassic to Cretaceous). The Vallonetto unit is characterized by a Briançonnais-type succession including marble and dolomitic-marble of Triassic age followed by Jurassic to Cretaceous calcschist. The Chaberton-Grand Hoche-Grand Argentier unit, belonging to the Pre-Piedmont zone, is formed by a thick dolomitic succession of Norian age followed by Rhaetian-Hettangian calcareous schists and then unconformable overlaid by prevailing calcschists with phyllites and beds of breccias (Jurassic to Cretaceous). The Piemonte-Liguria Oceanic units are formed by thick sequences of Upper Jurassic (?)–Cretaceous calcschist containing levels of micaschist and phylladic schist and embedding bodies of ophiolites (serpentinite, metabasite). Masses of gypsum and of carbonate breccias (Carniole Auct.) occur along the main tectonic contacts.

During the Quaternary, the Susa valley was carved with typical U-shaped cross section by the action of the glacier and, in its upper part, glacial deposits are recognizable on the valley flanks. Following the retreat of glaciers, several deep-seated gravitational slope deformations (DSGSD) developed on the valley flanks.

#### Data availability

The data used in this paper can be classified into two main categories: (1) landslide inventory and (2) thematic GIS-based maps. Data were collected using freely accessible and available datasets in national and regional geodatabases. Since the RES approach applied to debris flow requires the identification of environmental predisposing factors, thematic GIS-based maps were drawn starting from the available spatial datasets. Compared to the original version proposed by the authors (Bonetto et al. 2021), in this study, ten predisposing factors were considered for the definition of the DfPI (Table 1): bedrock lithology, quaternary deposits, lineament density, slope angle, curvature, elevation, slope aspect, channel network, landslide activity and land use. For the sake of simplicity, these factors are grouped into geological, geomorphological and hydrogeological parameters and land use.

Data management and analysis were conducted by using the QGIS software (v. 3.16.14 Bucuresti).

**Table 1** Spatial dataset of predisposing factors and type format detail

Spatial dataset	Predisposing factor	GIS type	Scale or resolution (Px)
Italian Geological Survey (CARG Project, Italian: Progetto Carta Geologica) at 1:50,000 scale	Bedrock lithology	Raster & Polygon	1:50,000 Px=5×5 m
	Quaternary deposits		
Digital Elevation Model DEM	Slope angle	Raster	Px=5×5 m
	Curvature		
	Elevation		
	Slope aspect		
BDTRE 2018 — Piemonte Channel Network	Channel network	Raster & Polygon	1:10,000 Px=5×5 m
SIFRAP — Landslide archive of Piemonte Region (Arpa Piemonte)	Landslide activity	Polygon	1:10,000 Px=5×5 m
Land Use Piemonte Region	Land use	Raster	1:10,000 Px=5×5 m
Orthophoto (WMS service) (resolution 30×30 cm <sup>2</sup> )	Lineament density	Raster	Px=5×5 m
	Detection of source area inventory (update)	Point	
RiskNat geoportal — Arpa Piemonte	Source area inventory	Point	

Source link:

- Piemonte Region Geodatabase — <http://www.geoportale.piemonte.it/>, last access 2022

- Regional Environmental Agency — ARPA — <http://webgis.arpa.piemonte.it/geoportale/>, last access 01/2022

- Regional Environmental Agency — ARPA — <http://webgis.arpa.piemonte.it/risknat/index.php/cat-news-nasc/402-pubblicata-la-base-dati-transfrontaliera-advitam-delle-frane-sullo-spazio-alcotra>, last access 10/2021

## Landslide inventory and source area archive

Debris flow source areas were available in the RiskNat–Arpa Piemonte inventory that contains events occurred (among other) in the Upper Susa Valley from 1990 to 2015. The original source area map was updated by manually adding recent events, easily identifiable from the analysis of the past aerial photographs between 2017 and 2018. An amount of 846 points of debris flow source area were recorded in 390 km<sup>2</sup> in the study area (Fig. 2).

### Predisposing factors

Geological parameters: bedrock lithology, quaternary deposits, lineament density

The geology of Upper Susa Valley was derived by the Foglio 132–152–153 Bardonecchia at 1:50,000 scale (Polino et al. 2002) of the official Italian Geological Cartography project (Fig. 3). The shapefiles of bedrock lithologies, quaternary deposits and landslides were converted into raster formats with 5 × 5-m cell resolution.

Based on the differences in strength and permeability of rocks and deposits and the presence of landslides, five classes for bedrock

lithology and five classes for quaternary deposits were identified (Bonetto et al. 2021) (Table 2).

Geological discontinuities (i.e. fractures, faults and foliations) induce a decrease in the mechanical strength of rock mass and increase the capacity to produce loose debris (Ferrero et al. 2016; Caselle et al. 2020; Umili et al. 2020). A regional map of the rock fracturing degree with a traditional survey is not feasible, and consequently, the general condition of the rock masses can be described by remote extraction of the main lineaments (Tripathi et al. 2000; Jordan et al. 2005; Vaz et al. 2012; Bonetto et al. 2015; Umili et al. 2018). Lineament extraction can be realized through automatic or manual approach from digital elevation model or orthophotos. In the automatic approach, the linear traces are detected on a DTM by algorithms based on principal curvature values (Bonetto et al. 2015, 2017) while in manual approach the user manually detects and tracks the lineaments. In this paper, manual lineament extraction was performed from visual interpretation of the orthophotos to increase lineament extraction accuracy, only focusing on bedrock outcrop areas. The track density map was derived (Fig. 3B) by using the Line Density tool on QGIS. This tool allows the measurement, within a given circular area, of the line density for each raster cell. This measure is obtained as the sum

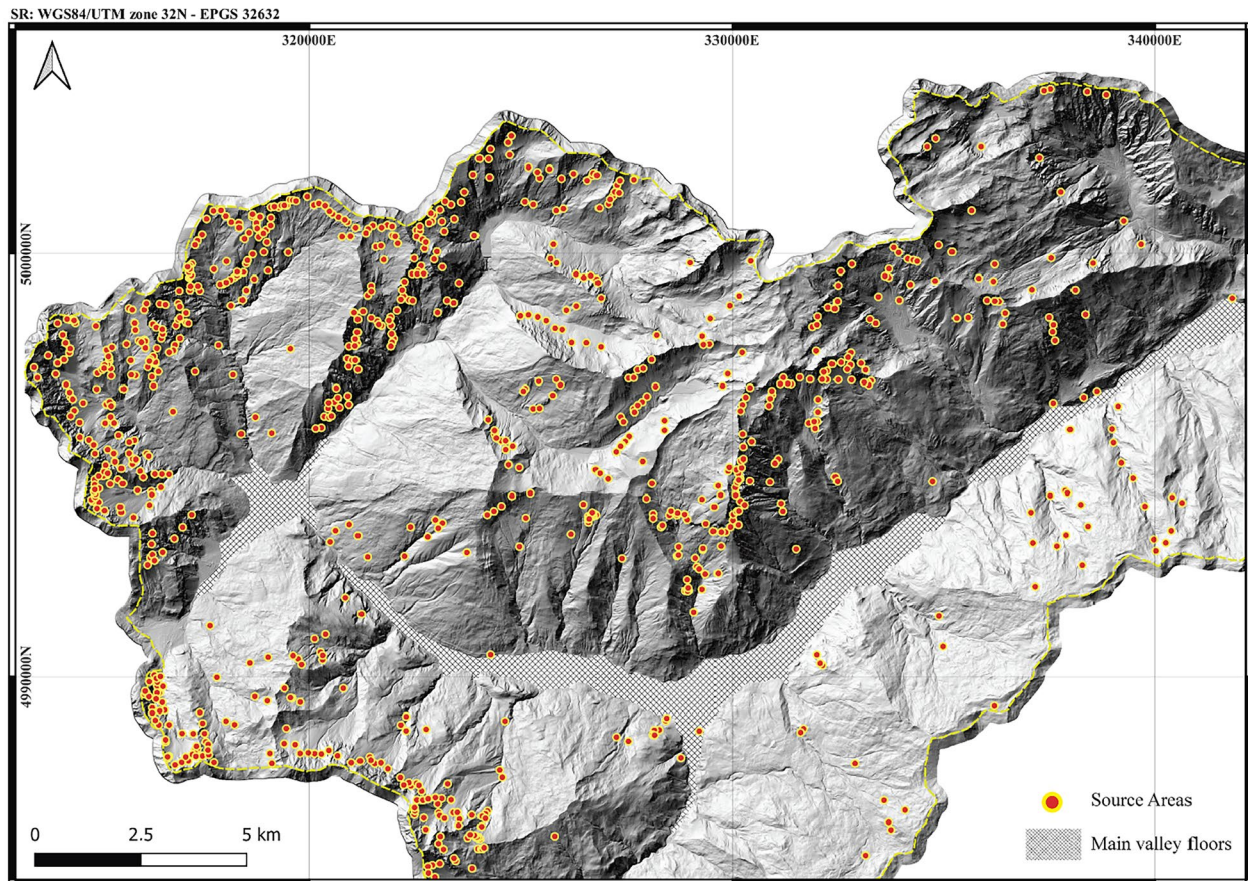


**Fig. 2** Location of the 846 debris flow source areas (red dots) recorded and detected in the Upper Susa Valley

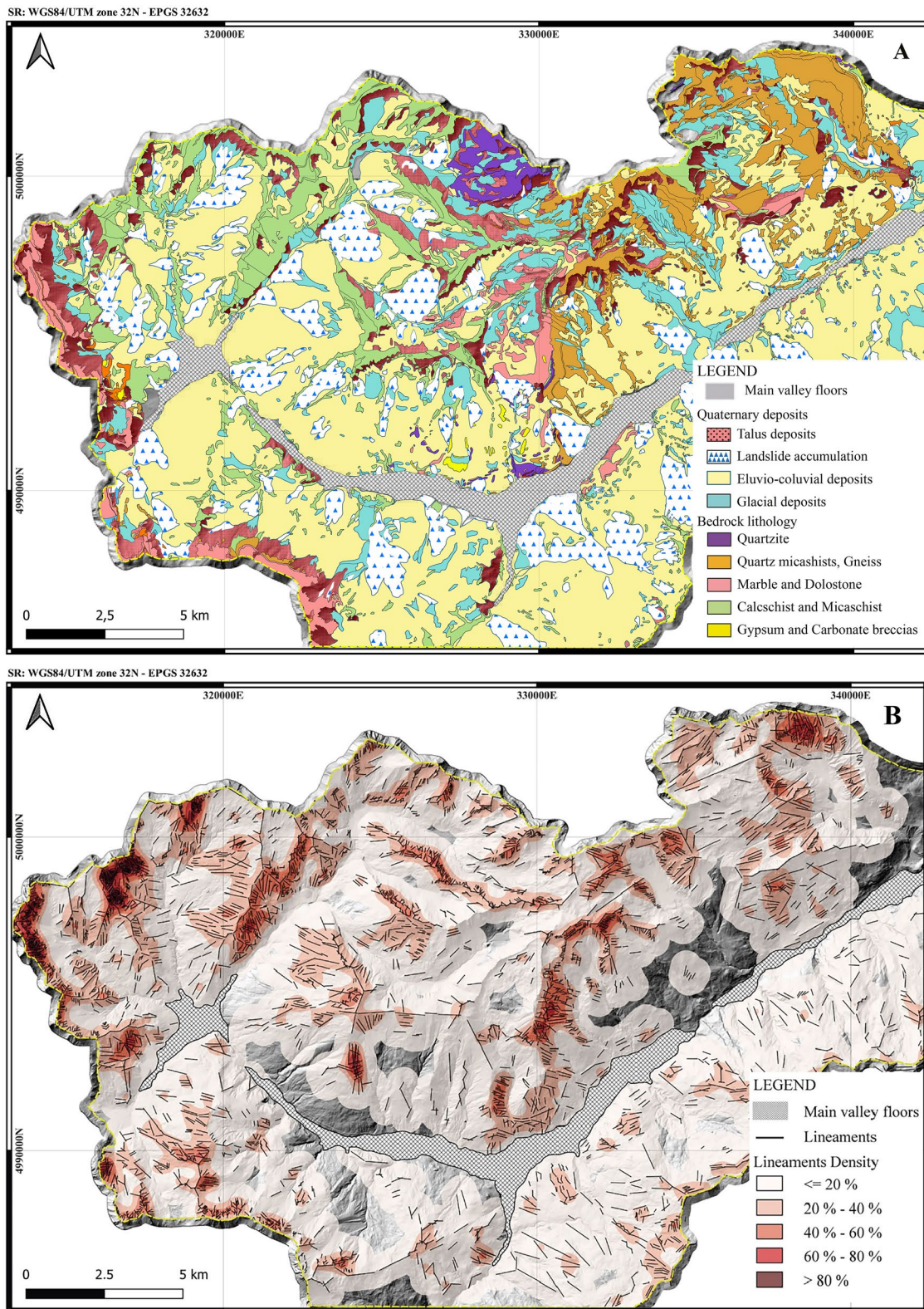


**Fig. 3** **A** Bedrock lithology and Quaternary deposits (modified from Polino et al. 2002). **B** The lineaments density maps developed from ortho-photo analysis

**Table 2** Categories for bedrock lithologies and quaternary deposits based on lithological and geotechnical similarities

Bedrock lithology
Quartzite
Quartz micaschist, gneiss
Marble and dolostone
Calcschist and micaschist
Gypsum and carbonate breccias
Quaternary deposits
Talus deposits
Eluvio-colluvial deposits
Glacial deposits
Landslide deposits

of all the line segments that intersect the circular area, divide to the area.

Geomorphological parameters: slope angle, curvature, elevation, slope aspect, landslide activity

The geomorphological layers were obtained from the DEM analysis using specific tools freely available in QGIS software. The resulting maps are shown in Fig. 4.

Slope angle is the result of the combined influence of many agents (Huma and Radulescu 1978; Carrara 1983; Maharaja 1993; Rozos et al. 2008) and is one of the predisposing factors capable of triggering debris flows. Slopes ranging between 20 and 45° (Takahashi 1981; Hungr et al. 1984; Rickenmann and Zimmermann 1993) are characteristic values for source area location. Five different slope classes were selected (Fig. 4A) for the classification of the study areas: (i) 0–8°, (ii) 8–15°, (iii) 15–25°, (iv) 25–35°, (v) > 35°.

The terrain curvature is the curvature of a line formed by intersecting a plane with the terrain surface. Operatively, the curvature value is the reciprocal of the radius of curvature of the line. Debris flows generally start where curvature is concave (Wieczorek et al. 1997; Delmonaco et al. 2003) and the flow can be channelled into gullies. Consequently, a distinction between concave (negative values), convex (positive values) and flat surface (values near zero) was made (Fig. 4B).

Elevation (Fig. 4C) and slope aspect (exposition) (Fig. 4D) do not directly influence the slope failure, but they are the result of tectonic activity and erosion process related to climatic condition (Rozos et al. 2008). The elevation was distinguished into classes with an elevation step of 500 m. In alpine regions, source areas are usually located at high elevation where deposits are concentrated.

The slope aspect reflects the exposition that is responsible for different local microclimatic conditions and solar exposition during the day. The exposition was classified with a step of 60° starting from the north (0 value).

The landslide activity map (Fig. 4E) shows the landslide distribution (not only debris flow but also every landslide type) and

their state of activity: (i) active, (ii) quiescent, (iii) inactive and (iv) not defined. In these areas, the overall rock mass and deposit conditions might increase the loose material availability that could be mobilized during a flow event.

Hydrological parameter: distance from channel network

Debris flow events require a channel to flow downstream. The flow erodes the channel leaves and banks, which are important sources of material available during the event. Usually, the areas prone to supplying material are located at distances lower than 200 m, while beyond these values the probability decrease (Rozos et al. 2008). For this reason, five different buffer zones were created to identify the distance along the river where material can be mobilized during the flow: (i) 0–50 m, (ii) 50–100 m, (iii) 100–150 m, (iv) 150–200 m, (v) > 200 m (Fig. 5).

Land use condition: land use

The land use describes the vegetational, mechanical and hydrological characteristics that control the slope stability (Glade 2003; Reichenbach et al. 2004). The land use influences the soil behaviour during rainfall and the magnitude of potential mobilizable material. The dataset, in raster format, provided by the regional archive allows five classes to be identified: (i) grassland, (ii) lakes, (iii) high forest, (iv) low forest, (v) rock and deposits (Fig. 6). This classification reflects the different soil conditions related to erodibility or resilience to the impact of rainfall.

### The RES methodology

The RES was proposed by Hudson in 1992. The methodology is based on a matrix approach that allows the numerical encoding of mutual interactions between the predisposing factors arranged along the diagonal terms ( $P_i$ ) of the matrix (Fig. 7). Off-diagonal terms ( $I_{ij}$ ) are scored with values from 0 (no interaction) to 4 (critical interaction) using the Expert Semi-Quantitative method (ESQ) (Harrison and Hudson 2006; Vagnon et al. 2015). The contribution of each parameter to the debris flow triggering is described by the weighting coefficient  $a_i$ :

$$a_i = \frac{1}{4} \left[ \frac{C + E}{\sum C + \sum E} \right] \cdot 100 \quad (1)$$

where C is the sum of the values in each row (Cause – C) and it represents the influence of the parameter  $P_i$  on the system, E is the sum of the values in each column (Effect – E) and it represents the influence of the system on parameter  $P_i$ .

The debris flow susceptibility index (DfPI) is given by:

$$DfPI = \sum (a_i \cdot P_{ik}) \quad (2)$$

where  $a_i$  is the weighting coefficient calculated for each parameter using Eq. 1, and  $P_{ik}$  corresponds to a specific value between 0 and 4 attributed to each class of the identified predisposing factors. The 0 value represents the most stable conditions (lower debris flow susceptibility) while the 4 value represents the most favourable conditions for debris flow triggering. The  $P_{ik}$  value describes the weight assigned to each predisposing factor based on its propensity to induce instability (Mazzoccola and Hudson 1996; Rozos et al. 2008, 2011).

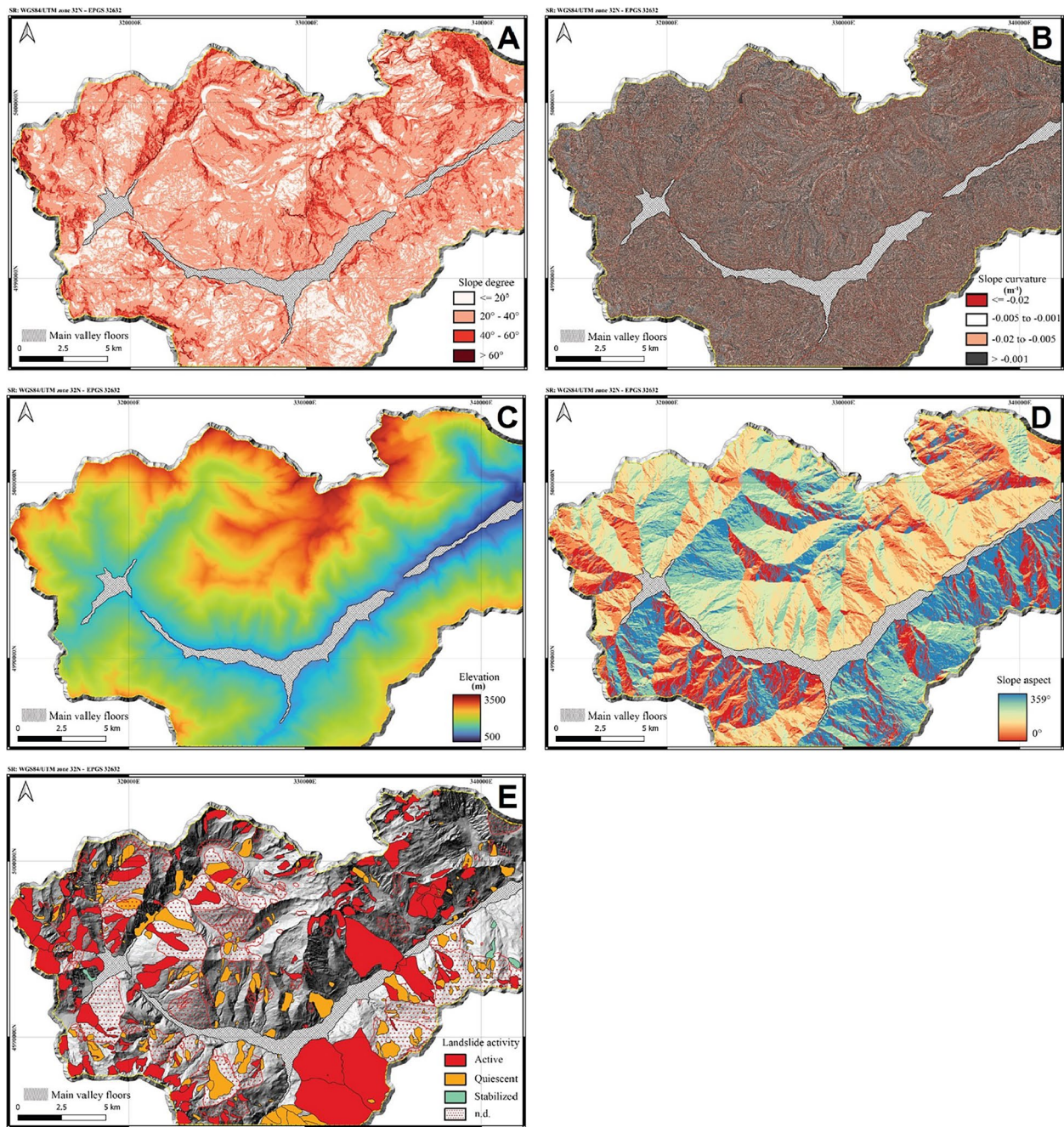


**Fig. 4** Geomorphological parameter maps of the Upper Susa Valley: **A** slope angle, **B** terrain curvature, **C** elevation, **D** slope exposition and **E** landslide activity

In this paper, an upgraded version of the Bonetto et al. (2021) approach is proposed to develop a GIS-based debris flow susceptibility map for the whole Upper Susa Valley by using a 5 × 5-m resolution grid. Curvature, land use and landslide activities were considered as predisposing factors in addition to those of the original version: lithology, fracture network, quaternary deposits, slope and

channel network. Two interaction matrices were created to separately analyse the mutual interaction between the bedrock lithology (matrix A) or deposits (matrix B) and the other parameters.

The GIS-based DfPI has the same range of values of the original DfPI version (from 0 to 100). Five susceptibility classes were defined by using a modified version of Brabb's susceptibility scale: low (0–20),

SR: WGS84/UTM zone 32N - EPSG 32632

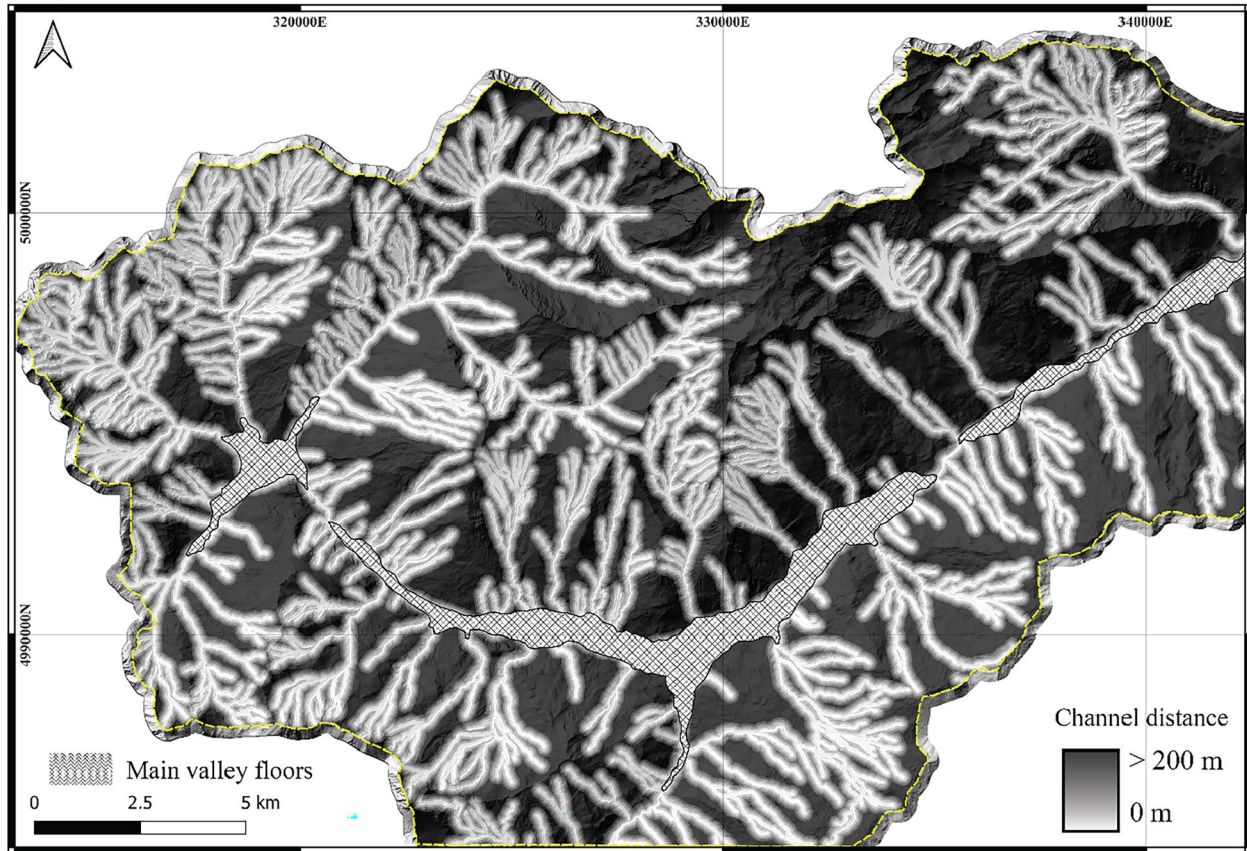


**Fig. 5** Channel network and buffer with distance from channel

medium (20–40), high (40–60), very high (60–80) and extreme (80–100).

## Result

### RES results

The off-diagonal terms of each matrix were coded considering the mutual influence between the parameters and  $a_i$  were calculated respectively for matrix A (bedrock lithologies) and matrix B (quaternary deposits) (Tables 3 and 4). By applying Eq. 2 to each grid cell and analysing separately bedrock outcrop areas and quaternary deposits (Table 5), the map of the whole study area was obtained (Fig. 8). The RES method highlights that debris flow susceptibility zones are concentrated at high elevation and where talus deposits are present. In addition, a large concentration of high susceptibility areas near the channel network and along the slope is emphasized. The NW sector has the areas with the highest susceptibility values compared to the rest of the valley. In fact, these sectors are characterized by the presence of deformed dolomitic rocks affected by intense post-metamorphic brittle deformation, as highlighted by the presence of the high amount of talus deposits.

The basins analysed in Bonetto et al. (2021) and their correspondent global DfPI are highlighted in Fig. 8. The results highlight that (i) qualitatively, there is a good agreement between the global DfPI and the grid DfPIs and (ii) the grid DfPI allows the direct identification of the areas capable of triggering debris flow events, providing great advantages especially for the planning of risk management activities.

### Comparison with other susceptibility methods and quantitative validation of the RES

Qualitative and preliminary analysis of the proposed RES approach is promising for the identification of the areas of the Upper Susa Valley most susceptible to debris flow triggering. However, for evaluating the reliability of this procedure, highlighting its potentialities and limitations, RES was firstly compared with two well-established susceptibility methods available in the scientific literature: the Regional Qualitative Heuristic Susceptibility Mapping (RQHSM) and the Likelihood Ratio (LR). Then, for a quantitative comparison and for evaluating the effectiveness of the RES, the RQHSM and the LR, the prediction rate approach (Chung and Fabbri 2003) was used. Figure 9 shows the logical steps followed for the quantitative comparison between the susceptibility mapping methods analysed in this work.

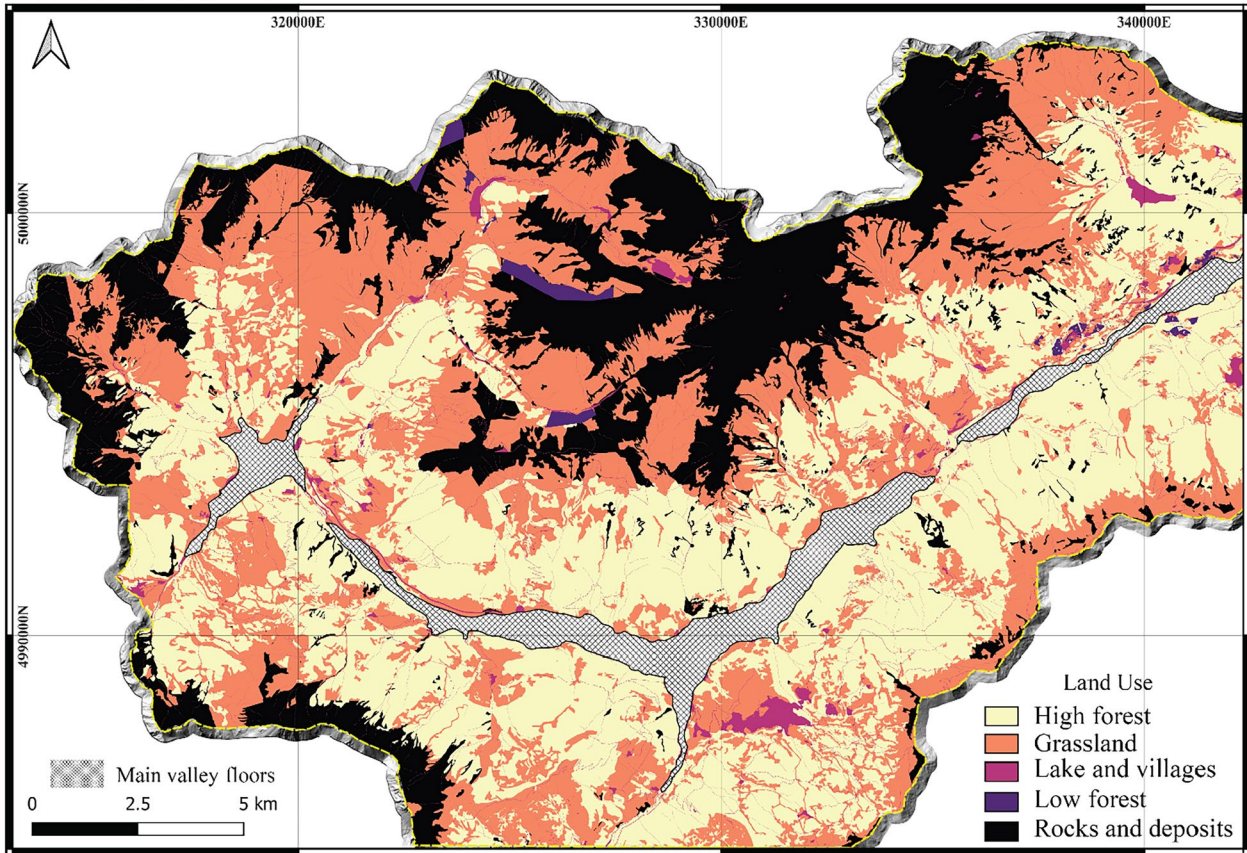


Fig. 6 Land use map

**The RQHSM — regional qualitative heuristic susceptibility mapping**

The RQHSM is a heuristic method that allows defining a susceptibility index (SI) by scoring the predisposing factors using geological and

geomorphologic criteria (Soeters and van Westen 1996; Riopel et al. 2006; Blais-Stevens et al. 2010, 2011, 2012, 2014 and references herein). For each parameter, different classes were defined, according to the propensity of triggering debris flows (Table 6). Following the equation proposed by Blais-Stevens and Behnia (2016), SI was calculated as:

Fig. 7 Structure of the interaction matrix and principal operations. Off-diagonal terms and  $P_{ik}$  values are reported

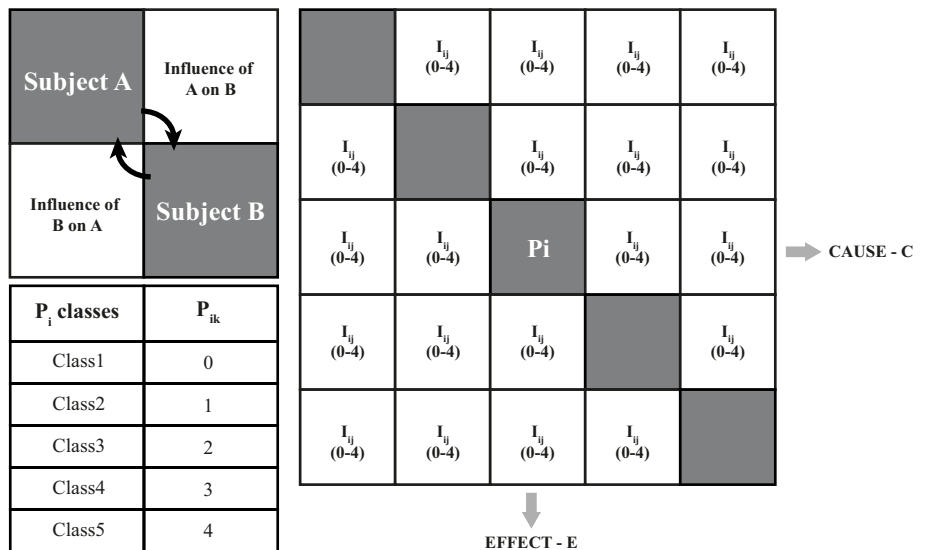


**Table 3** The interaction matrix encoded for bedrock lithologies outcrop (matrix A)

Matrix A — bedrock lithologies									
a/a	1	2	3	4	5	6	C	C + E	a <sub>i</sub>
1	<b>Bedrock lithology</b>	2	3	0	1	1	7	11	2.70
2	0	<b>Slope</b>	4	2	3	0	9	22	5.39
3	0	3	<b>Channel network</b>	2	2	0	7	23	5.64
4	0	2	4	<b>Curvature</b>	2	1	9	16	3.92
5	1	2	1	2	<b>Land use</b>	0	6	15	3.68
6	3	4	4	1	1	<b>Lineament density</b>	13	15	3.68
<b>E</b>	4	13	16	7	9	2	51	102	

$$SI = 0.2 \cdot G + 0.3 \cdot S1 + 0.05 \cdot S2 + 0.3 \cdot D + 0.15 \cdot C \quad (3)$$

with geology (G), slope angle (S1), slope aspect (S2), drainage system (D) and plan curvature (C). The resulting debris flow susceptibility map is shown in Fig. 10. For a direct comparison with DfPI values, SIs were multiplied by 100 and classified following the same criteria.

The RQHSM highlights the areas near the drainage system with a high probability of failure, considering that the onset of debris flows is usually triggered in steep streams. In this case, only the materials into the stream and along the riverbanks are detected as susceptible at triggering phenomena.

#### The likelihood ratio (LR)

The likelihood ratio (Lee 2004; Lee and Pradhan 2007; Demir et al. 2015 and references herein) is a statistical method that correlates

environmental conditions with landslide areas and extends the landslides spatial occurrence in similar setting areas.

Based on the assumption that future landslides will occur under the same conditions as past landslides, the statistical method allows defining which factors, or combination of factors, play a fundamental role in the landslide initiation. With the LR, it is possible to evaluate the relationship between the dependent parameter (landslide occurrence) and the independent parameter (such as geological, geomorphological and hydrogeological features) and retrieve a ratio between the landslide occurrence probability and the non-occurrence probability calculated for each class factor. For debris flow analysis, these terms correspond to the ratio between:

$$FR = \frac{\text{Landslide occurrence ratio}}{\text{Area domain}} \quad (4)$$

where the landslide occurrence ratio is the ratio between the number of landslides in i-th class and the total amount of landslide in study

**Table 4** The interaction matrix encoded for Quaternary deposits outcrop (matrix B)

Matrix B — quaternary deposits									
a/a	1	2	3	4	5	6	C	C + E	a <sub>i</sub>
1	<b>Quaternary deposits</b>	2	2	2	1	2	10	25	3.77
2	4	<b>Slope</b>	4	2	3	3	18	33	4.97
3	3	3	<b>Channel network</b>	2	2	3	16	31	4.67
4	2	2	4	<b>Curvature</b>	2	1	15	29	4.37
5	1	2	1	2	<b>Land use</b>	1	12	28	4.22
6	4	4	1	2	3	<b>Landslide activity</b>	20	20	3.01
<b>E</b>	15	15	15	14	16	16	91	166	

**Table 5** Classification and scores of the predisposing factors considered in the interaction matrices A and B for the RES application

Matrix A — bedrock lithology				Matrix B — Quaternary deposits			
Parameter	Class	$P_{ik}$	$P_{ik} \times a_i$	Parameter	Class	$P_{ik}$	$P_{ik} \times a_i$
Bedrock lithology	Quartzites	0	0	Quaternary deposits	No deposit	0	0
	Gneiss, quartz micaschist	1	2.7		Talus deposits	1	3.77
	Marble and dolostone	2	5.39		Glacial deposits	2	7.53
	Calcschist and micaschist	3	8.09		Landslide deposits	3	11.3
	Gypsum and carbonate breccias	4	10.78		Eluvio-colluvial deposits	4	15.06
Slope	0–8°	0	0	Slope	0–8°	0	0
	8–15°	1	5.39		8–15°	1	4.97
	15–25°	2	10.78		15–25°	2	9.94
	25–35°	3	16.18		25–35°	3	14.91
	> 35°	4	21.57		> 35°	4	19.88
Channel network	0–50 m	4	22.55	Channel network	0–50 m	4	18.67
	50–100 m	3	16.91		50–100 m	3	14.01
	100–150 m	2	11.27		100–150 m	2	9.34
	150–200 m	1	5.64		150–200 m	1	4.67
	> 200 m	0	0		> 200 m	0	0
Curvature	Concave	4	15.69	Curvature	Concave	4	17.47
	Flat	1	3.92		Flat	1	4.37
	Convex	3	11.76		Convex	3	13.1
Land use	Villages, urban	0	0	Land use	Villages, Urban	0	0
	High forests	1	3.68		High forests	1	4.22
	Low forests	2	7.35		Low forests	2	8.43
	Grassland	3	11.03		Grassland	3	12.65
	Rock and deposits	4	14.71		Rock and deposits	4	16.87
Lineament density	Weak	0	0	Landslide activity	--	0	0
	Moderate	1	3.68		Nd	1	3.01
	Strong	2	7.35		Stabilized	2	6.02
	Very strong	3	11.03		Quiescent	3	9.04
	Intense	4	14.71		Active	4	12.05

area, the area domain is the ratio between the area of i-th class and the total area in our case study. If the FR is greater than 1, it means that factor class has a high correlation with the event and vice versa.

Operatively, for evaluating the FR, the landslide inventory described in the “[Landslide inventory and source area archive](#)” section, was randomly divided into two sets in the proportion 70% (593)–30% (253): the training and the validation sets (Fig. 11). The

training set was used to build the statistical model, while the validation set was used to validate the results.

Using Eq. 4, the FR values were calculated for each layer class (Table 7). The susceptibility index for each cell was obtained as the sum of all the FRs calculated for each selected parameter:

$$SI = \sum FR \quad (5)$$

SR: WGS84/UTM zone 32N - EPSG 32632

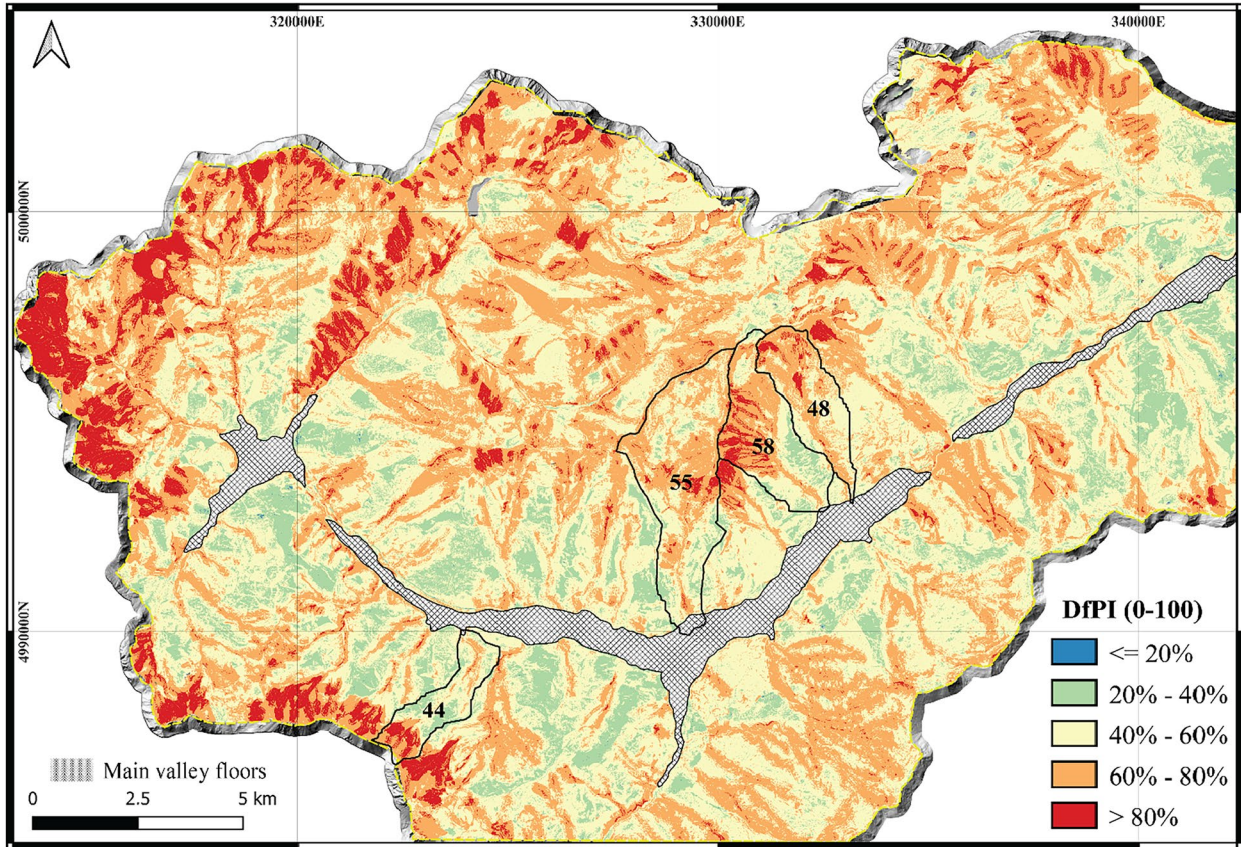


**Fig. 8** Landslide susceptibility maps obtained with the RES method. The basin bounded by black continuous lines refers to the basin studied in Bonetto et al. (2021). The black numbers are the global DfPIs evaluated for those basins

and the resulting debris flow susceptibility map is shown in Fig. 12. SI values were scaled up to vary between 0 and 100 for a direct comparison with DfPIs and SIs from the RQHSM.

The LR method highlights three areas with high susceptibility values ( $> 80$ ) located in the southwestern and central parts of the study area. These areas correspond to the high-altitude zones at the peaks and the crests of the mountain chain and to large areas occupied by detrital materials and talus deposits. In these areas, the structural setting of the rock masses (made of prevailing marble-dolostone and calcschist) and their mechanical proprieties are favourable for producing a huge amount of loose material. Along the slope and in presence of the forests, the susceptibility values are low while the presence of talus deposits is noted as the most critical areas. These low values are attributed to high slope areas and zones in proximity to the channel network focusing on the areas with coarse deposits and high fractured rocks.

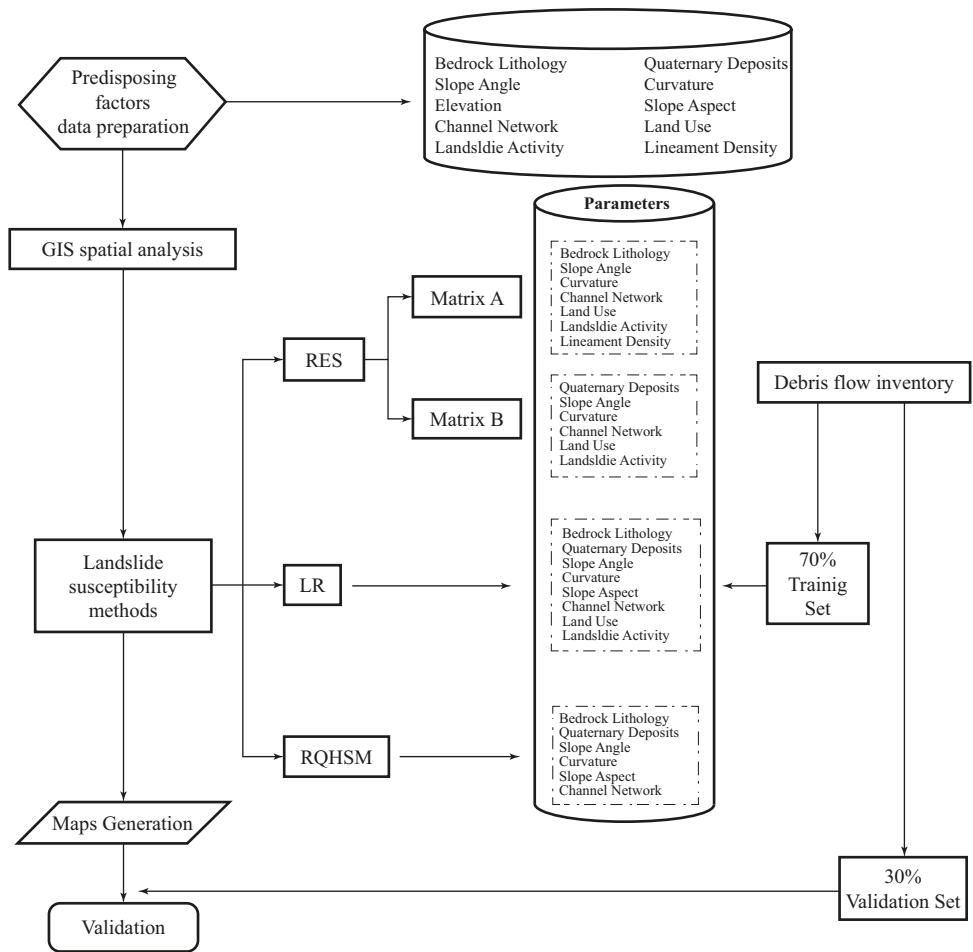
### Model validation

In the previous section, a visual and qualitative comparison was made between the RES and the other models. In this section, quantitative analyses were performed to assess the validity of

the three susceptibility methods. However, the assessment of the model robustness is always a challenging task. Many authors have proposed different methodologies for the comparison between forecasted results and observed data. In this study, the susceptibility maps were validated by using the Prediction Rate Curve (Chung and Fabbri 2003). This approach is based on the direct comparison between the source area estimated from susceptibility maps and the real source area from debris flow inventory. The validation set consists of 253 landslide source areas (30% of total source areas inventory) previously excluded from the statistical model analysis. The source area was overlaid on the susceptibility maps (Fig. 13) and the validation phase was performed plotting the LSI value in x-axis and the cumulate percentage of landslides on y-axis (Fig. 14).

The use of the same validation dataset for all three methodologies allows the direct comparison between the curves obtained and the evaluation of their robustness. The validation step verifies that the maximum number of landslides was included in the highest susceptibility classes. Results show that the landslide areas predicted by the RES method in the high-extreme susceptibility range (50–100) are 96% while in the same range, the performance

**Fig. 9** Workflow used for the comparison and validation of the methods analysed



of the RQHSM and LR methods is 82% and 77%. This means that in the RES methodology most landslides were predicted in areas characterized by high-extreme susceptibility while, in contrast,

in the other methods more landslides were predicted in areas of low–high susceptibility. This fact reflects a lower prediction capability.

**Table 6** Debris flow parameters and class ratings for the RQHSM method

Geology		Distance from channel network			
Classes	Rating	Classes	Rating		
Eluvio-colluvial and talus deposits	1	0–50 m	1		
Glacial deposits	0.7	50–100 m	0.75		
Landslide deposits	0.5	100–150 m	0.5		
Bedrock lithology	0.1	150–200 m	0.25		
		> 200 m	0		
Slope angle (°)		Slope aspect (°)		Curvature (1/m)	
Classes [°]	Rating	Classes [°]	Rating	Classes [1/m]	Rating
0–8	0.1	0–45	0.1	< –0.02	1
8–15	0.5	45–135	0.5	–0.02 to 0.005	0.8
15–25	1	135–225	1	0.005 to 0.001	0.5
25–35	0.5	225–315	0.5	> 0.001	0.1
> 35	0.1	315–360	0.1		

SR: WGS84/UTM zone 32N - EPSG 32632

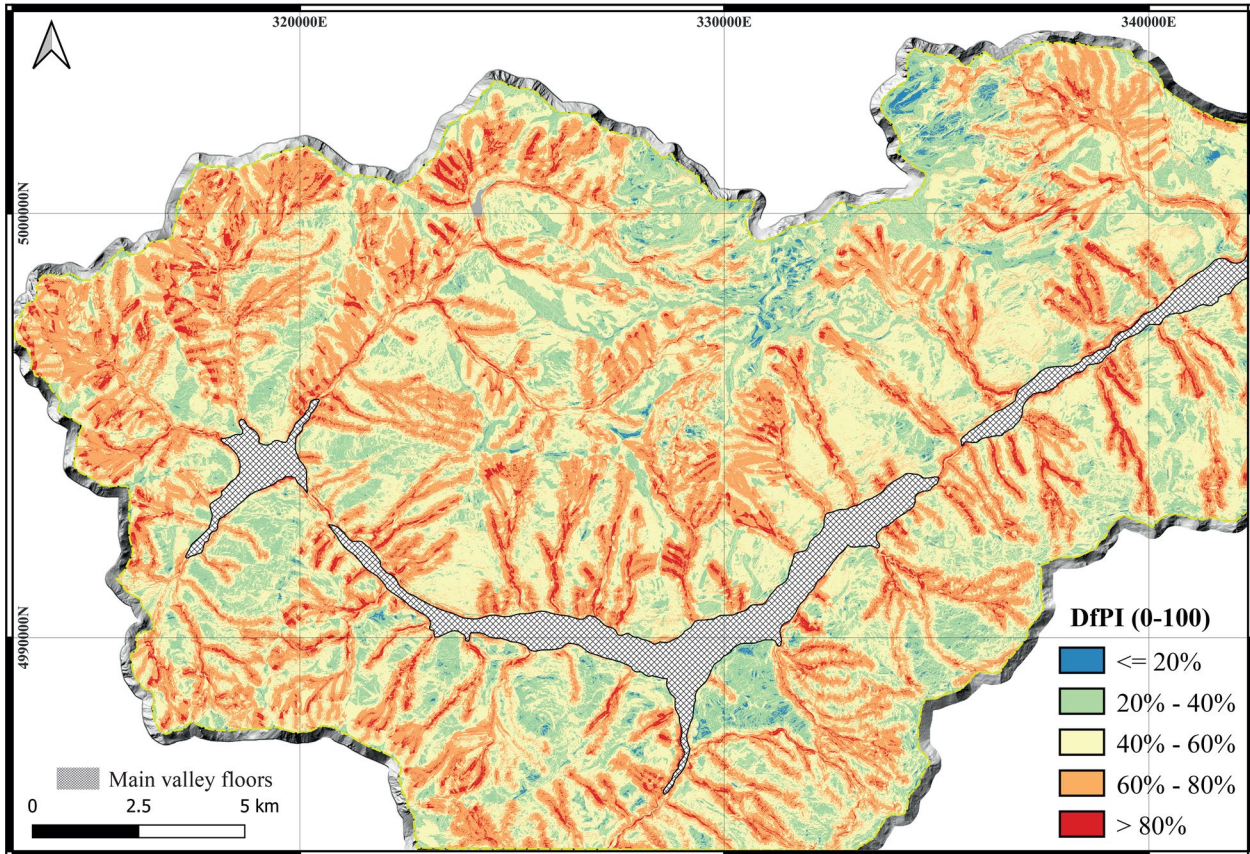


**Fig. 10** Landslide susceptibility maps obtained by the RQHSM method

### Discussion

Using predisposing parameters selected from national and regional geodatabases, debris flow susceptibility maps were developed using the RES, RQHSM and LR methods. Analysis of the prediction curves (Fig. 14) shows the trend differences between the analysed methodologies: the RES appears to be more accurate in predicting susceptible areas based on debris flow database analysis. To compare and evaluate the models, the percentage of the areas classified as susceptible is reported in Fig. 15. In the RES and RQHSM methods, the differences in the percentage of susceptible areas are negligible (0.2|0.8 Low, 13.2|17.7 Medium, 47.0|43.8 High, 33.3|32.2 Very high, 6.3|5.5 Extreme). These two methodologies classify most of the territory with high and very high susceptibility while, on the other hand, the LR approach identifies a different proportion of areas with respect to the other two methods (25.3 Low, 44.2 Medium, 16.8 High, 10.2 Very high, 3.3 Extreme). In this case, the LR method identifies few areas of high susceptibility by concentrating high values in a small portion of the area. The difference is also appreciable comparing the maps in Fig. 13, which shows the overlay of the

susceptibility map and the location of the source areas used in the validation process.

A common feature of all three methods is that the spatial distribution of the most susceptible areas corresponds to the zone of maximum elevation with the presence of debris along the slope and steep sections. The RQHSM and RES methods identify the channel network as playing a significant role in the triggering phenomena, while the LR method highlights highly fractured outcrop rocks as a key factor. The low susceptibility zone was detected in the alluvial planes and flat areas, but the same susceptibility class in the LR was also detected along the slope and near channels.

The applicability of different methods to debris flow susceptibility depends on several factors (e.g. amount and quality of the data) but established standards and codes of practice are not available for the choice of the most appropriate method for landslide susceptibility evaluation.

The LR method is based on the evaluation of the relationships between predisposing factors (thematic layers) and the distribution of debris flow source areas collected in the past years (landslide inventory).

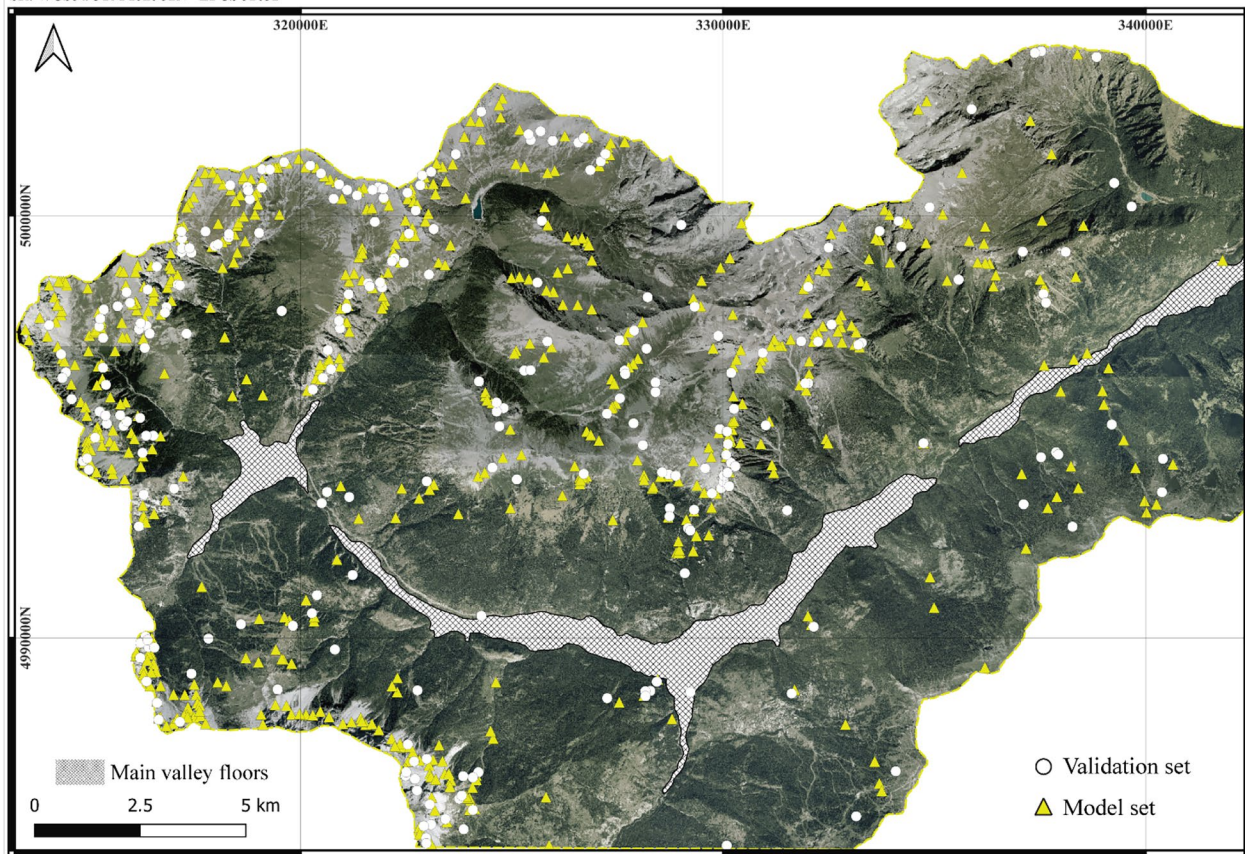


**Fig. 11** The validation (circles) and the model (yellow triangles) sets in which the landslide inventory was randomly divided

Thus, a detailed landslide archive is a necessary input to apply the methodology. In remote mountain areas, where it is difficult to collect information, some events may be missed, and this issue can lead to an underestimation of the potential triggering areas with a consequent decrease in forecasting quality. The application of remote sensing survey can redress this problem, but the precise time of occurrence and the definition of magnitude remain undetectable. This information is not required for landslide susceptibility, but it is fundamental for hazard or risk assessment. Moreover, the visual detection of source areas has some limitations due to the misclassification of landslide events and underestimation of the number of events recorded. The growth of vegetation and action of snow and glaciers could partially or totally delete the evidence of past events. In addition, the complex terrain morphologies may not allow the proper identification of the source area if the quality of aerial photography is not sufficiently detailed.

The evaluation of landslide susceptibility requires geological, morphological and statistical input data to process the analysis. Much

effort is required to collect and validate the necessary input data, which are not always available from open-access geo-environmental databases. Statistical methods need the available spatial-temporal datasets of landslide events. The RES and RQHSM methodologies are essentially based on predisposing parameters derived from geological, morphological and hydrogeological thematic layers.

In the RES methodology proposed, starting from available databases, several geological, geo-structural, morphological and hydrographic parameters were considered to quantify their mutual interaction and to define a debris flow susceptibility map. In particular, the parameters for the different lithological classes of the bedrock and for their degree of fracturing were quantified in the regional-scale tectonic setting, and for the Quaternary deposits.

The RES method, as applied in this study, proved to be low-cost and time-saving and allowed sectors with different propensities to triggering debris flow to be identified.

**Table 7** The likelihood values

Parameter	Class	Area in the domain (km <sup>2</sup> )	% of domain	No. of landslide	% of landslide*	FR
<b>Slope</b>	0–8°	23.11	7.92	3	0.51	0.06
	8–15°	33.94	17.44	8	1.35	0.08
	15–25°	96.40	31.18	36	6.07	0.19
	25–35°	131.84	30.17	169	28.50	0.94
	> 35°	101.48	9.12	377	63.58	6.97
<b>Geology</b>	Calcschist	32.16	8.36	152	25.63	3.06
	Marble and dolostone	10.69	2.78	61	10.29	3.70
	Quartz-micaschist, gneiss	26.40	6.87	39	6.58	0.96
	Quartzite	3.95	1.03	1	0.17	0.16
	Gypsum and carbonate breccias	0.62	0.16	2	0.34	2.10
	Glacial deposits	67.17	17.47	39	6.58	0.38
	Talus deposits	30.53	7.94	174	29.34	3.69
	Landslide deposits	22.79	5.93	25	4.22	0.71
	Eluvio-colluvial deposits	189.05	49.18	92	15.51	0.32
<b>Distance from channel network</b>	0–50 m	84.24	21.76	235	39.63	1.82
	50–100 m	67.76	17.51	120	20.24	1.16
	100–150 m	51.74	13.37	92	15.51	1.16
	150–200 m	39.56	10.22	50	8.43	0.82
	> 200 m	143.75	37.14	96	16.19	0.44
<b>Elevation</b>	< 1000 m	11.99	3.10	7	1.18	0.38
	1000–1500 m	85.07	21.99	13	2.19	0.10
	1500–2000 m	110.02	28.44	90	15.18	0.53
	2000–2500 m	107.75	27.86	283	47.72	1.71
	2500–3000 m	62.67	16.20	195	32.88	2.03
	> 3000 m	9.34	2.41	5	0.84	0.35
<b>Land use</b>	Villages, Urban	17.30	4.49	17	2.87	0.64
	Grassland	131.50	34.14	123	20.74	0.61
	Low forest	2.12	0.55	6	1.01	1.84
	High forest	158.53	41.16	55	9.27	0.23
	Rocks and deposits	75.70	19.65	392	66.10	3.36
<b>Slope aspect</b>	< 60°	56.15	14.54	85	14.33	0.99
	60–120°	55.59	14.40	154	25.97	1.80
	120–180°	80.30	20.80	171	28.84	1.39
	180–240°	65.80	17.04	95	16.02	0.94
	240–300°	58.14	15.06	41	6.91	0.46
	> 300°	70.08	18.15	47	7.93	0.44

**Table 7** (continued)

Parameter	Class	Area in the domain (km <sup>2</sup> )	% of domain	No. of landslide	% of landslide*	FR
<b>Landslide activity</b>	Active	79.01	33.22	216	52.43	1.58
	n. d	122.68	51.58	120	29.13	0.56
	Quiescent	35.40	14.88	76	18.45	1.24
	Stabilized	0.74	0.31	0	0.00	0.00
<b>Curvature (m<sup>-1</sup>)</b>	< -0.02	45.28	11.72	28	4.72	0.40
	-0.02 to -0.005	84.72	21.93	156	26.31	1.20
	-0.005 to -0.001	157.89	40.88	115	19.39	0.47
	> -0.001	98.36	25.47	294	49.58	1.95

\*Total number of landslides is 593 (training sets)

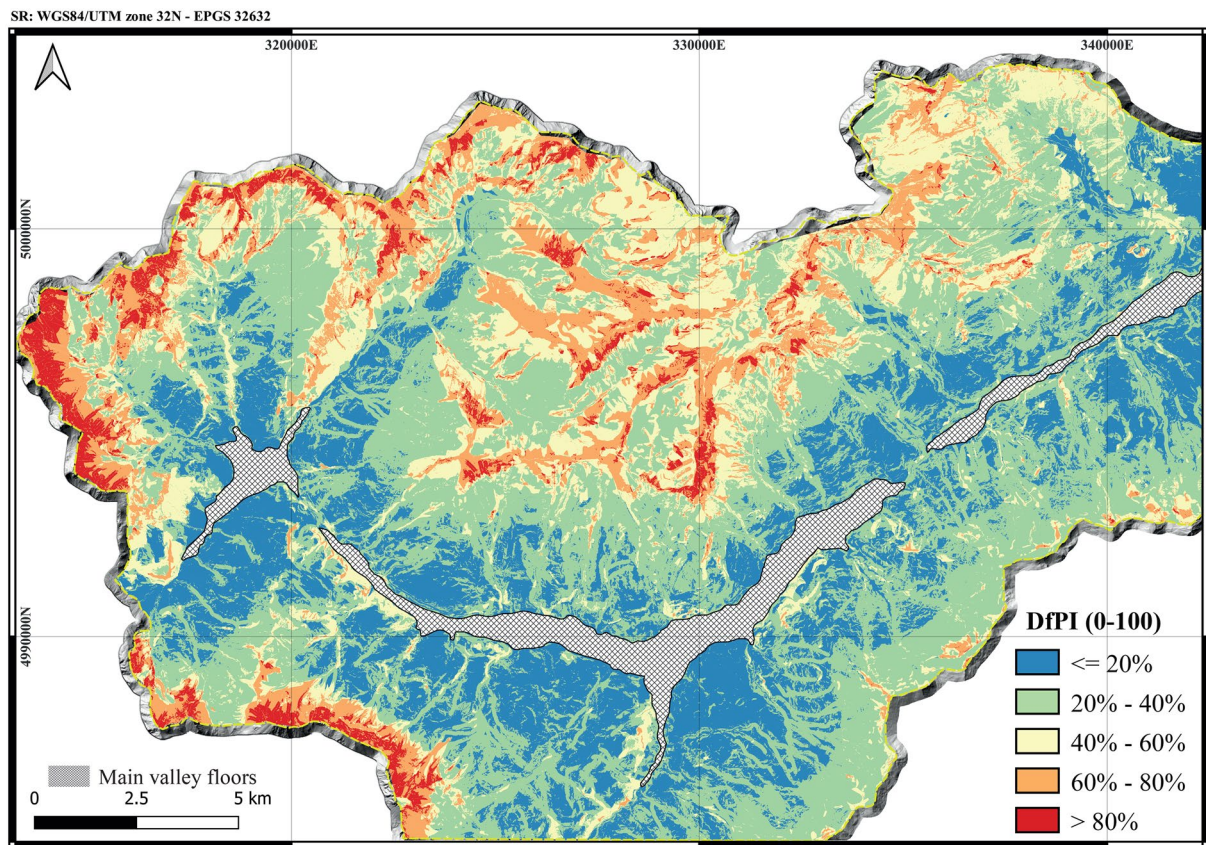


**Fig. 12** Landslide susceptibility map obtained by the LR method

**Fig. 13** Overlay among susceptibility maps and the validation set: **a** the RES, **b** the RQHSM and **c** the LR methods

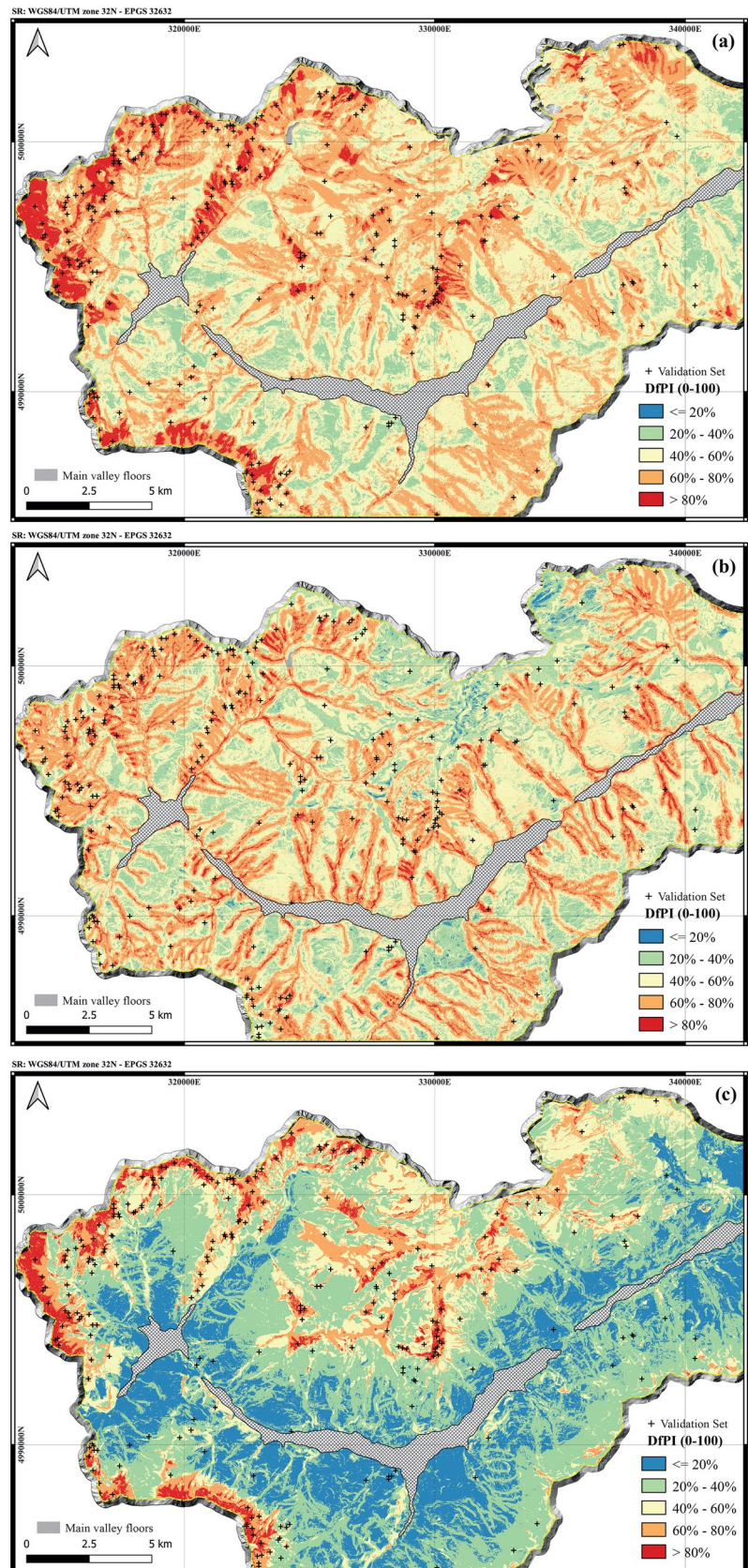


**Fig. 14** Prediction rate curve using 253 debris flow source areas from the landslide inventory

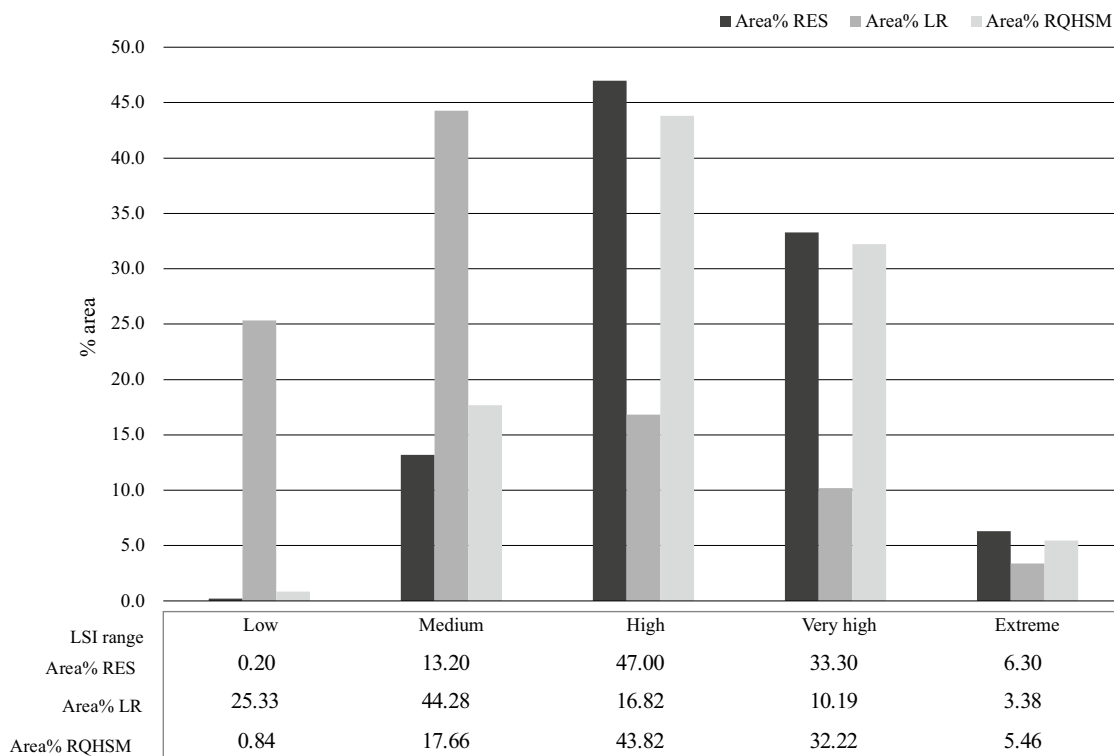
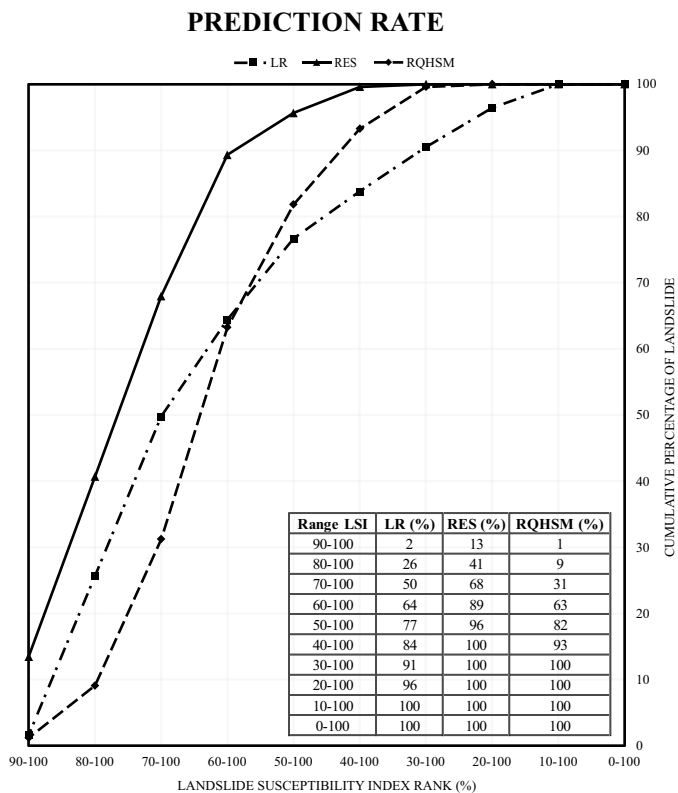


**Fig. 15** Percentage of areas classified by using the RES (dark grey bars), RQHSM (medium grey bars) and LR (light bars) methods that fall in each susceptibility class

## Conclusions

Susceptibility analysis in mountain areas is the first step in the risk assessment procedure. It is useful for local authorities to define potential areas that could be affected by debris flow phenomena. Different methodologies for susceptibility analyses are available in the scientific literature, but which to choose depends on the scale of analysis required and the amount and quality of available data.

In this work, an innovative GIS-based application of Rock Engineering System (RES) was used for debris flow susceptibility mapping. Starting from the definition of a global DfPI for a single debris flow basin, as suggested by Bonetto et al. (2021), in this paper, a debris flow susceptibility map of the Upper Susa Valley (W Alps, Italy) was developed with a 5 × 5-m grid resolution. Important updates to the Bonetto et al. (2021) approach were proposed: (i) new predisposing factors, such as land use, landslide activity and other geomorphological aspects, were considered; (ii) two interaction matrices were proposed for considering the mutual interaction of the bedrock lithology or deposits with the other parameters; (iii) GIS-based mapping with evaluation of DfPI for each cell of the grid.

The susceptibility map obtained was compared with the RQHSM and LR methods. Numerical quantification of the validity of the susceptibility forecasting was performed by using the Prediction Rate Curve model, comparing the susceptibility model results with an available debris flow source inventory. In general, there was a good agreement between the forecasted and observed source areas. However, the RES-based map appears to be the most efficient and robust in the detection of source areas, since it was able to predict 96% of the source areas that fall into the high-extreme susceptibility range (50–100).

The study demonstrates that the application of the RES method offers an opportunity for initial debris flow susceptibility screening at medium and large scale, using available and open-access data, and meets the needs of authorities for land use management and planning. Further studies will be devoted to a comparison with other more sophisticated and complex methodologies (e.g. multivariate statistical approach or artificial neural network methods) developed in recent years.

## Acknowledgements

We thank the Editor and two anonymous reviewers for their constructive comments. We want to acknowledge Mr. Ian Charles Lister from the Language Centre (CLA) of the Politecnico di Torino for his precious help in the English editing.

## Funding

Open access funding provided by Università degli Studi di Torino within the CRUI-CARE Agreement.

## Declarations

**Conflict of interest** The authors declare no competing interests.

**Open Access** This article is licensed under a Creative Commons Attribution 4.0 International License, which permits use, sharing, adaptation, distribution and reproduction in any medium or format, as long as you give appropriate credit to the original author(s) and the source, provide a link to the Creative Commons licence, and indicate if changes were made. The images or other third party

material in this article are included in the article's Creative Commons licence, unless indicated otherwise in a credit line to the material. If material is not included in the article's Creative Commons licence and your intended use is not permitted by statutory regulation or exceeds the permitted use, you will need to obtain permission directly from the copyright holder. To view a copy of this licence, visit <http://creativecommons.org/licenses/by/4.0/>.

## References

- Abella EC, Van Westen CJ (2008) Spatial landslide risk assessment in Guantánamo province, Cuba. In *Landslides and engineered slopes, from the past to the future: proceedings of the 10th international symposium on landslides and engineered slopes ISL*, 30 June–4 July 2008, Xian, China (pp 1879–1885)
- Akgun A (2012) A comparison of landslide susceptibility maps produced by logistic regression, multi-criteria decision, and likelihood ratio methods: a case study at İzmir, Turkey. *Landslides* 9:93–106. <https://doi.org/10.1007/s10346-011-0283-7>
- Aleotti P, Chowdhury R (1999) Landslide hazard assessment: summary review and new perspectives. *Bull Eng Geol Environ* 58(1):21–44. <https://doi.org/10.1007/s100640050066>
- Alvioli M, Baum RL (2016) Parallelization of the TRIGRS model for rainfall-induced landslides using the message passing interface. *Environ Model Softw* 81:122–135
- Anagnostopoulos GG, Burlando P (2012) An Object-oriented computational framework for the simulation of variably saturated flow in soils, using a reduced complexity model. *Environ Model Softw* 38:191–202
- Baum RL, Godt JW (2010) Early warning of rainfall-induced shallow landslides and debris flows in the USA. *Landslides* 7(3):259–272
- Blais-Stevens A, Lipovsky P, Kremer M, Couture R, Page A (2011) Landslide inventory and susceptibility mapping for a proposed pipeline route, Yukon Alaska Highway Corridor, in: *Proceedings of the Second World Landslide Forum*, Rome, Italy, 362, (ESS Cont. # 20110101)
- Blais-Stevens A, Lipovsky P, Kremer M, Couture R, Smith S (2012) Landslide inventory and susceptibility mapping for the Yukon Alaska Highway Corridor, In: *Proceedings of the 11th International and 2nd North American Symposium on landslides and engineered slopes*, Banff, Alberta, 1:777–782
- Blais-Stevens A, Couture R, Page A, Koch J, Clague J, Lipovsky P (2010) Landslide susceptibility, hazard and risk assessments along pipeline corridors in Canada, In: *Proceedings of the 63rd Canadian geotechnical conference and 6th Canadian permafrost conference*, Calgary (AB), 878–885
- Blais-Stevens A, Kremer M, Bonnaventure PP, Smith SL, Lipovsky P, Lewkowicz AG (2014) Active layer detachment slides and retrogressive thaw slumps susceptibility mapping for present-day and projected climate conditions along the Yukon Alaska Highway Corridor. A qualitative heuristic approach, In: *Proceedings of the Engineering Geology for Society and territory, IAEG conference*, Torino, Springer, 1:449–453, (GSC Contribution: 20130369)
- Blais-Stevens A, Behnia P (2016) Debris flow susceptibility 494 mapping using a qualitative heuristic method and Flow-R along the Yukon Alaska Highway Corridor, Canada. *Nat Hazard* 16(2):449–462
- Bonetto S, Facello A, Ferrero AM, Umili G (2015) A tool for semi-automatic linear feature detection based on DTM. *Comput Geosci* 75:1–12
- Bonetto S, Facello A, Umili G (2017) A new application of curvatool semi-automatic approach to qualitatively detect geological lineaments. *Environ Eng Geosci* 23:179–190. <https://doi.org/10.2113/gseengeosci.23.3.179>
- Bonetto S, Mosca P, Vagnon F, Vianello D (2021) New application of open source data and Rock Engineering System for debris flow susceptibility analysis. *J Mt Sci* 18. <https://doi.org/10.1007/s11629-021-6814-3>
- Brabb EE (1987) Innovative approaches to landslide hazard and risk mapping. *Int J Rock Mech Min Sci Geomech Abstr* 24:A16. [https://doi.org/10.1016/0148-9062\(87\)91363-5](https://doi.org/10.1016/0148-9062(87)91363-5)

- Carrara A (1983) Multivariate models for landslide hazard evaluation. *Math Geol* 15:403–426
- Carrara A (1984) Landslide hazard mapping: aim and methods. *Mouvements de terrains; Communications du 7 colloque, Caeu, 22–24 Mars, Documents du BRGM* 83:141–151
- Carrara A, Cardinali M, Guzzetti F, Reichenbach P (1995) GIS technology in mapping landslide hazard. In: Carrara A, Guzzetti F (eds) *Geographical Information Systems in Assessing Natural Hazards*. Kluwer Academic Publisher, Dordrecht, The Netherlands, pp 135–175
- Carrara A, Guzzetti F, Cardinali M, Reichenbach P (1999) Use of GIS technology in the prediction and monitoring of landslide hazard. *Nat Hazards* 20(2):117–135
- Carrara A, Crosta G, Frattini P (2008) Comparing models of debris-flow susceptibility in the alpine environment. *Geomorphology* 94:353–378
- Caselle C, Bonetto S, Costanzo D (2020) Crack coalescence and strain accommodation in gypsum rock. *Frattura Ed Integrità Strutturale* 14(52):247–255
- Chacón J, Irigaray C, Fernandez T, El Hamdouni R (2006) Engineering geology maps: landslides and geographical information systems. *Bull Eng Geol Env* 65(4):341–411
- Chung C, Fabbri AG (2003) Validation of 522 Spatial Prediction Models for Landslide Hazard Mapping. *Nat Hazards* 30:451–472
- Clerici A, Perego S, Tellini C, Vescovi P (2002) A procedure for landslide susceptibility zonation by the conditional analysis method. *Geomorphology* 48(4):349–364. [https://doi.org/10.1016/S0169-555X\(02\)00079-X](https://doi.org/10.1016/S0169-555X(02)00079-X)
- Corominas J, Copons R, Vilaplana JM et al (2003) Integrated Landslide Susceptibility Analysis and Hazard Assessment in the Principality of Andorra. *Nat Hazards* 30:421–435. <https://doi.org/10.1023/B:NHAZ.0000007094.74878.d3>
- Corominas J, van Westen C, Frattini P et al (2014) Recommendations for the quantitative analysis of landslide risk. *Bull Eng Geol Environ* 73:209–263. <https://doi.org/10.1007/s10064-013-0538-8>
- Costa JE, Jarrett RD (1981) Debris flows in small mountain stream channels of Colorado and their hydrological implications. *Bulletin of the Association of Engineering Geology* 18:309–322
- Cruden DM, Varnes DJ (1996) Landslide types and processes, in landslides. In: Turner AK, Schuster RL (eds) *Investigation and Mitigation*. Special Report, vol 247. Transport Research Board, National Research Council, Washington D.C.
- Dai FC, Lee CF (2001) Terrain-based mapping of landslide susceptibility using a geographical information system: a case study. *Can Geotech J* 38:911–923
- Dal Piaz GV (2010a) The Italian Alps: a journey across two centuries of Alpine geology. *J Virtual Explor* 36(8):77–106
- Dal Piaz GV, Gianotti F, Monopoli B, Pennacchioni G, Tartarotti P, Schiavo A (2010b) Note illustrative della Carta Geologica d'Italia alla scala 1:50.000. Note Illus. Della Cart. Geol. D'Italia alla scala 1:50.000
- Delmonaco G, Leoni G, Margottini C, Puglisi C, Spizzichino D (2003) Large scale debris-flow hazard assessment: a geotechnical approach and GIS modelling. *Nat Hazard* 3:443–455
- Demir G, Aytekin M, Akgun A (2015) Landslide susceptibility mapping by frequency ratio and logistic regression methods: an example from Niksar-Resadiye (Tokat, Turkey). *Arab J Geosci* 8(3):1801–1812
- Fell R, Corominas J, Bonnard C, Cascini L, Leroi E, Savage WZ (2008) Guidelines for landslide susceptibility, hazard and risk zoning for land-use planning. *Eng Geol* 102(3–4):99–111
- Ferrero AM, Migliazza MR, Pirulli M, Umili G (2016) Some open issues on rockfall hazard analysis in fractured rock mass: problems and prospects. *Rock Mech Rock Eng* 49(9):3615–3629
- Glade T (2003) Landslide occurrence as a response to land use change: a review of evidence from New Zealand. *CATENA* 51(3–4):297–314
- Guzzetti F, Carrara A, Cardinali M, Reichenbach P (1999) Landslide hazard evaluation: a review of current techniques and their application in a multi-scale study, Central Italy. *Geomorphology* 31:181–216. [https://doi.org/10.1016/S0169-555X\(99\)00078-1](https://doi.org/10.1016/S0169-555X(99)00078-1)
- Guzzetti F, Galli M, Reichenbach P, Ardizzone F, Cardinali M (2006a) Landslide hazard assessment in the Collazzone area, Umbria, central Italy. *Nat Hazard Earth Syst Sci* 6:115–131. <http://dx.doi.org/10.5194/nhess-6-115-2006a>
- Guzzetti F, Reichenbach P, Ardizzone F, Cardinali M, Galli M (2006b) Estimating the quality of landslide susceptibility models. *Geomorphology* 81:166–184. <https://doi.org/10.1016/j.geomorph.2006.04.007>
- Harrison JP, Hudson JA (2006) Comprehensive hazard identification in rock engineering using interaction matrix mechanism pathways. In: *Proceedings of the 41st U.S. Rock Mechanics Symposium - ARMA's Golden Rocks 2006 - 50 Years of Rock Mechanics*
- Huabin W, Gangjun L, Weiya X, Gonghui W (2005) GIS-based landslide hazard assessment: an overview. *Prog Phys Geogr* 29(4):548–567
- Hudson JA (1992) *Rock Engineering Systems: Theory & Practice*, High Plains Press (JAH), Chicester, UK
- Huma I, Radulescu D (1978) Automatic production of thematic maps of slope stability. *Bull IAEG* 11(17):95–99
- Hung O, Morgan GC, Kellerhals R (1984) Quantitative analysis of debris torrent hazards for design of remedial measures. *Can Geotech J* 21(4):663–677
- Hung O (2005) Classification and terminology. In *Debris-flow hazards and related phenomena* (pp. 9–23). Springer, Berlin, Heidelberg
- Hung O, Leroueil S, Picarelli L (2014) The Varnes classification of landslide types, an update. *Landslides* 11:167–194
- Hutchinson JN (1988) Morphological and geotechnical parameters of landslides in relation to geology and hydrogeology. In: Bonnard Ch (ed) *Landslides*. *Proceedings 5th International Conference on Landslides, Lausanne, vol 1* pp 3–35
- Hutchinson JN (1992) Keynote paper: Landslide hazard assessment. In: Bell DH (ed) *Proceedings of the 6th International Symposium on Landslides*. Christchurch, New Zealand, Vol 3 pp 1805–1841
- IAEG (1990) Suggested nomenclature for landslides. International Association of Engineering Geology Commission on Landslides. *Bulletin IAEG* 13–16 No. 41
- Iverson RM (1997) The physics of debris flows. *Rev Geophys* 35(3):245–296
- Iverson RM (2014) Debris flows: behaviour and hazard assessment. *Geology Today* 30(1)
- Jakob M, Hung O (2005) Debris-flow hazards and related phenomena, vol 739. Springer, Berlin
- Jordan G, Meijninger BML, Van Hinsbergen DJJ et al (2005) Extraction of morphotectonic features from DEMs: Development and applications for study areas in Hungary and NW Greece. *Int J Appl Earth Obs Geoinf* 7:163–182. <https://doi.org/10.1016/j.jag.2005.03.003>
- Kanungo DP, Sarkar S, Sharma S (2011) Combining neural network with fuzzy, certainty factor and likelihood ratio concepts for spatial prediction of landslides. *Nat Hazards* 59(3):1491–1512. <https://doi.org/10.1007/s11069-011-9847-z>
- Kim MK, Yoo YI, Song JJ (2008) Methodology to quantify rock behavior around shallow tunnels by rock engineering systems. *Geosystem Eng* 11:37–42. <https://doi.org/10.1080/12269328.2008.10541283>
- Lee S (2004) Application of likelihood ratio and logistic regression models to landslide susceptibility mapping using GIS. *Environ Ma Nag* 34(2):223–232. <https://doi.org/10.1007/s00267-003-0077-3>
- Lee S, Pradhan B (2007) Landslide hazard mapping at Selangor, Malaysia using frequency ratio and logistic regression models. *Landslides* 4(1):33–41
- Maharaja RJ (1993) Landslides processes and landslide susceptibility analysis from an upland watershed: a 27 case study from St. Andrew, Jamaica. *West Indies Eng Geol* 34:53–79
- Malusà M, Mosca P (2002) Assetto strutturale duttile dei livelli superiori del Massiccio d'Ambin (Alpi Occidentali). In: *Guida all'escursione pre-Riunione: Il sistema Alpino-Appenninico nel Cenozoico (6–9 settembre 2002)*. Riunione della 81° Riunione della Società Geologica Italiana, Torino, Italia (10–12 settembre). pp 83–86
- Malusa M, Mosca P, Borghi A et al (2002) Approccio multidisciplinare per la ricostruzione dell'assetto tettono-stratigrafico e dell'evoluzione metamorfico-strutturale di un settore di catena orogenica; l'esempio dell'Alta Valle di Susa (Alpi occidentali). In: *Tra Alpi, 608 Dinaridi e Adriatico; Atti dell'80 (super a) riunione estiva della Società Geologica Italiana*
- Mazzoccola DF, Hudson JA (1996) A comprehensive method of rock mass characterization for indicating natural slope instability. *Q J Eng Geol* 29:37–56. <https://doi.org/10.1144/GSL.QJEGH.1996.029.P1.03>
- Meten M, Bhandary NP, Yatabe R (2015) Application of GIS-based fuzzy logic and rock engineering system (RES) approaches for landslide

- susceptibility mapping in Selelkula area of the Lower Jema River Gorge, Central Ethiopia. *Environ Earth Sci* 74:3395–3416
- Montgomery DR, Dietrich WE (1994) A physically based model for the topographic control on shallow landsliding. *Water Resour Res* 30(4):1153–1171
- Nachbaur A, Rohmer J (2011) Managing expert-information uncertainties for assessing collapse susceptibility of abandoned underground structures. *Eng Geol* 123(3):166–178
- Pereira S, Zezere JL, Bateira C (2012) Technical Note: Assessing predictive capacity and conditional independence of landslide predisposing factors for shallow landslide susceptibility models. *Nat Hazards Earth Syst Sci* 12:979–988. <https://doi.org/10.5194/nhess-12-979-2012>
- Piana F, Fioraso G, Iracea A et al (2017) Geology of Piemonte region (NW Italy, Alps–Apennines interference zone). *J Maps* 13(2):395–405
- Polino R, Dela Pierre F, Borghi A et al (2002) Note illustrative della Carta Geologica d'Italia alla scala 1:50.000, Foglio 132–152–153 Bardonecchia della Carta Geologica d'Italia - Regione Piemonte, Direzione Regionale dei servizi Tecnici di Prevenzione. Litografia Geda, Nichelino (TO) Italia.
- Pokharel B, Althwaynee OF, Aydda A et al (2021) Spatial clustering and modelling for landslide susceptibility mapping in the north of the Kathmandu Valley. *Nepal Landslides* 18:1403–1419
- Regmi N, Giardino J, Vitek J (2010) Modeling susceptibility to landslides using the weight of evidence approach: Western Colorado, USA. *Geomorphology* 115:172–187. <https://doi.org/10.1016/j.geomorph.2009.10.002>
- Reichenbach P, Galli M, Cardinali M, Guzzetti F, Ardizzone F (2004) Geomorphological mapping to assess landslide risk: Concepts, methods and applications in the Umbria region of central Italy. *Landslide Hazard Risk*, 429–468
- Reichenbach P, Rossi M, Malamud BD, Mihir M, Guzzetti F (2018) A review of statistically-based landslide susceptibility models. *Earth Sci Rev* 180:60–91
- Rickenmann D, Zimmermann M (1993) The 1987 debris flows in Switzerland: documentation and analysis. *Geomorphology* 8:175–189
- Rigon R, Bertoldi G, Over TM (2006) GEOtop: A distributed hydrological model with coupled water and energy budgets. *J Hydrometeorol* 7(3):371–388
- Riopol S, Couture R, Tewari K (2006) Mapping susceptibility to landslides in a permafrost environment: case study in the Mackenzie Valley, Northwest Territories, GeoTech Event, Ottawa, Canada 18–21 June, 13 pp., 2006 Risk. *Bull Eng Geol Environ* 73:209–638 263. <https://doi.org/10.1007/s10064-013-0538-8>
- Rozos D, Bathrellos GD, Skillodimou HD (2011) Comparison of the implementation of rock engineering system and analytic hierarchy process methods, upon landslide susceptibility mapping, using GIS: a case study from the Eastern Achaia County of Peloponnesus, Greece. *Environ Earth Sci* 63:49–63. <https://doi.org/10.1007/s12665-010-0687-z>
- Rozos D, Pyrgiotis L, Skias S, Tsararatos P (2008) An implementation of rock engineering system for ranking the instability potential of natural slopes in Greek territory. An Application in Karditsa County Landslides 5:261–270. <https://doi.org/10.1007/s10346-008-0117-4>
- Simoni S, Zanotti F, Bertoldi G, Rigon R (2008) Modelling the probability of occurrence of shallow landslides and channelized debris flows using GEOtop-FS. *Hydrological Processes: an International Journal* 22(4):532–545
- Soeters R, van Westen CJ (1996) Slope instability recognition, analysis, and zonation, in: Landslides, investigation and mitigation. In: Turner AK, Schuster RL (eds) Transportation Research Board, National Research Council, Special Report 247. National Academy Press, Washington, DC, pp 129–177
- Sujatha ER, Rajamanickam V, Kumaravel P, Saranathan E (2013) Landslide susceptibility analysis using probabilistic likelihood ratio model—a geospatial-based study. *Arab J Geosci* 6(2):429–440. <https://doi.org/10.1007/s12517-011-0356-x>
- Tavoularis N, Koumantakis I, Rozos D, Koukis G (2017) The Contribution of Landslide Susceptibility Factors Through the Use of Rock Engineering System (RES) to the Prognosis of Slope Failures: An Application in Panagopoula and Malakasa Landslide Areas in Greece. *Geotech Geol Eng* 36:1491–1508
- Tavoularis N, Papathanassiou G, Ganas A, Argyrakos P (2021) Development of the Landslide Susceptibility Map of Attica Region, Greece, Based on the Method of Rock Engineering System. *Land* 10(2):148
- Takahashi T (1981) Estimation of potential debris flows and their hazardous zones; soft countermeasures for a disaster. *J Nat Dis Sci* 3:57–89
- Tiranti D, Bonetto S, Mandrone G (2008) Quantitative basin characterization to refine debris-flow triggering criteria and processes: An example from the Italian Western Alps. *Landslides* 5:45–57. <https://doi.org/10.1007/s10346-007-0101-4>
- Tiranti D, Cremonini R, Marco F, Gaeta AR, Barbero S (2014) The DEFENSE (debris Flows triggered by storms—nowcasting system): An early warning system for torrential processes by radar storm tracking using a Geographic Information System (GIS). *Comput Geosci* 70:96–109
- Tiranti D, Cremonini R, Asprea I, Marco F (2016) Driving factors for torrential mass-movements occurrence in the Western Alps. *Front Earth Sci* 4. <https://doi.org/10.3389/feart.2016.00016>
- Tripathi NK, Gokhale KVGK, Siddiqui MU (2000) Directional morphological image transforms for lineament extraction from remotely sensed images. *Int J Remote Sens* 21:3281–3292. <https://doi.org/10.1080/014311600750019895>
- Umili G, Bonetto S, Ferrero AM (2018) An integrated multiscale approach for characterization of rock masses subjected to tunnel excavation. *J Rock Mech Geotech Eng* 10:513–522. <https://doi.org/10.1016/j.jrmge.2018.01.007>
- Umili G, Bonetto S, Mosca P, Vagnon F, Ferrero AM (2020) In situ block size distribution aimed at the choice of the design block for rockfall barriers design: A case study along Gardesana road. *Geosciences* 10(6):223
- Vagnon F, Ferrero AM, Pirulli M, Segalini A (2015) Theoretical and experimental study for the optimization of flexible barriers to restrain Debris Flows. *Geingegneria Ambientale e Mineraria* 145(2):29–35
- van Asch TW, Malet JP, van Beek LP, Amitrano D (2007) Techniques, issues and advances in numerical modelling of landslide hazard. *Bulletin De La Société Géologique De France* 178(2):65–88
- van Westen CJ, van Asch TWJ, Soeters R (2006) Landslide hazard and risk zonation - Why is it still so difficult? *Bull Eng Geol Environ* 65:167–184. <https://doi.org/10.1007/s10064-005-0023-0>
- van Westen CJ, Castellanos E, Kuriakose SL (2008) Spatial data for landslide susceptibility, hazard, and vulnerability assessment: an overview. *Eng Geol* 102(3–4):112–131. <https://doi.org/10.1016/j.enggeo.2008.03.010>
- Varnes DJ (1978) Slope movement types and processes. In: Schuster RL, Krizek RJ (eds) Special Report 176: Landslides: Analysis and Control. TRB, National Research Council, Washington, D.C., pp 11–33
- Vaz DA, Di Achille G, Barata MT, Alves EI (2012) Tectonic lineament mapping of the Thaumasia Plateau, Mars: Comparing results from photointerpretation and a semi-automatic approach. *Comput Geosci* 48:162–172. <https://doi.org/10.1016/j.cageo.2012.05.008>
- Wang X, Zhang L, Wang S et al (2014) Regional landslide susceptibility zoning with considering the aggregation of landslide points and the weights of factors. *Landslides* 11:399–409
- Wieczorek GF, Mandrone G, DeCola L (1997) The Influence of Hillslope Shape on Debris-Flow Initiation. In: Engineering FICWR (ed) ASCE. Division, San Francisco, CA, pp 21–31
- Xiao T, Segoni S, Chen L et al (2020) A step beyond landslide susceptibility maps: a simple method to investigate and explain the different outcomes obtained by different approaches. *Landslides* 17:627–640

**Davide Vianello** (✉) · **Sabrina Bonetto**

Department of Earth Science, University of Torino, 10125 Turin, Italy  
Email: [davide.vianello@unito.it](mailto:davide.vianello@unito.it) [sabrina.bonetto@unito.it](mailto:sabrina.bonetto@unito.it)

**Federico Vagnon**

Department of Environment, Land and Infrastructure Engineering (DIATI), Politecnico di Torino, 10129 Turin, Italy  
Email: [federico.vagnon@polito.it](mailto:federico.vagnon@polito.it)

**Pietro Mosca**

Institute of Geosciences and Earth Resources, National Research Council (CNR), 10125 Turin, Italy  
Email: [pietro.mosca@cnr.it](mailto:pietro.mosca@cnr.it)